8-2013

THE MOLECULAR INTERACTION BETWEEN TYPE II DIABETES AND ALZHEIMER'S DISEASE THROUGH CROSS-SEEDING OF PROTEIN MISFOLDING

George A. Edwards III

THE MOLECULAR INTERACTION BETWEEN TYPE II DIABETES AND ALZHEIMER'S DISEASE THROUGH CROSS-SEEDING OF PROTEIN MISFOLDING

by

George Edwards III, B.S.

APPROVED:

_____
Claudio Soto, Ph.D., Advisory Professor

_____
Jaroslaw Aronowski, Ph.D.

_____
Andrew Bean, Ph.D.

_____
David Gorenstein, Ph.D.

_____
Anne Sereno, Ph.D.

_____

Approved:

_____
Dean, University of Texas
Graduate School of Biomedical Sciences at Houston

THE MOLECULAR INTERACTION BETWEEN TYPE II DIABETES AND ALZHEIMER'S DISEASE THROUGH CROSS-SEEDING OF PROTEIN MISFOLDING

A

Thesis

Presented to the Faculty of

The University of Texas

Health Science Center at Houston

and

The University of Texas

M.D. Anderson Cancer Center

Graduate School of Biomedical Sciences

in Partial Fulfillment

of the Requirements for the Degree of

MASTERS of SCIENCE

by

George Edwards III, B.S.

Houston, Texas

August 2013

Dedication

First and foremost, to my Lord and Savior Jesus Christ for giving me the abilities and opportunities to be where I am in my life. I am beyond blessed, and I am excited to see where my future progresses.

To my grandparents, my late grandmother Loretta Edwards and grandfather George Edwards, Sr. Thank you for pushing me to go further, teaching me to never settle, and loving me, even at the worst of times.

To my family and friends who have always believed in me and supported me.

To my past laboratory, currently at the University of Florida McKnight Brain Institute, Dr. Jennifer Bizon and Dr. Barry Setlow. I am grateful for you both engraving a love and interest to study the uniqueness of the brain, AD, and neuroscience.

To my post-doc mentor, Dr. Ines Moreno-Gonzalez. I cannot be happier that I can learn from and aspire to become an astonishing researcher, like you. You are always there when I need you for anything, and I am so blessed to have you in my life.

Acknowledgements

I would like to thank my mentor and advisor, Dr. Claudio Soto. Thank you for giving me the opportunity to research what I love and to be a part of an amazing laboratory family. Dr. Soto is such a great teacher, and I have learned so much from him.

I would like to thank Natalia Salvadores for all of her previous work on the project.

I would like thank my committee members, Dr. Jaroslaw Aronowski, Dr. Andrew Bean, Dr. David Gorenstein, Dr. Anne Sereno, and Dr. Claudio Soto. Thank you all for being so helpful and supporting; your supervision and participation is irreplaceable.

I would like to thank the Soto laboratory for all of the guidance and support. Each person is a special piece to the puzzle, and I am thankful for the opportunity to know each of you and call you all family.

I would like to acknowledge my friends and colleagues in the Neuroscience program here at UT Health Science Center in Houston. Thank you all for the kindness and all-around honest care you show fellow students. I know I can depend on you guys for anything.

THE MOLECULAR INTERACTION BETWEEN TYPE II DIABETES AND ALZHEIMER'S DISEASE THROUGH CROSS-SEEDING OF PROTEIN MISFOLDING

George Edwards III, B.S.

Thesis Advisor: Claudio Soto, Ph.D.

With the population of the world aging, the prominence of diseases such as Type II Diabetes (T2D) and Alzheimer's disease (AD) are on the rise. In addition, patients with T2D have an increased risk of developing AD compared to age-matched individuals, and the number of AD patients with T2D is higher than among aged-matched non-AD patients. AD is a chronic and progressive dementia characterized by amyloid-beta (Aβ) plaques, neurofibrillary tangles (NFTs), neuronal loss, brain inflammation, and cognitive impairment. T2D involves the dysfunctional use of pancreatic insulin by the body resulting in insulin resistance, hyperglycemia, hyperinsulinemia, pancreatic beta cell (β-cell) death, and other complications. T2D and AD are considered protein misfolding disorders (PMDs). PMDs are characterized by the presence of misfolded protein aggregates, such as in T2D pancreas (islet amyloid polypeptide - IAPP) and in AD brain (amyloid– Aβ) of affected individuals. The misfolding and accumulation of these proteins follows a seeding-nucleation model where misfolded soluble oligomers act as nuclei to propagate misfolding by recruiting other native proteins. Cross-seeding occurs when oligomers composed by one protein seed the aggregation of a different protein. Our hypothesis is that the pathological interactions between T2D and AD may in part occur through cross-seeding of protein misfolding. To test this hypothesis, we examined how each respective aggregate (Aβ or IAPP) affects the disparate disease pathology through *in vitro* and *in vivo* studies. Assaying Aβ aggregates influence on T2D pathology, $IAPP^{+/+}/APP_{Swe}{}^{+/-}$ double transgenic (DTg) mice exhibited exacerbated

T2D-like pathology as seen in elevated hyperglycemia compared to controls; in addition, IAPP levels in the pancreas are highest compared to controls. Moreover, $IAPP^{+/+}/APP_{Swe}^{+/-}$ animals demonstrate abundant plaque formation and greater plaque density in cortical and hippocampal areas in comparison to controls. Indeed, $IAPP^{+/+}/APP_{Swe}^{+/-}$ exhibit a colocalization of both misfolded proteins in cerebral plaques suggesting IAPP may directly interact with Aβ and aggravate AD pathology. In conclusion, these studies suggest that cross-seeding between IAPP and Aβ may occur, and that these protein aggregates exacerbate and accelerate disease pathology, respectively. Further mechanistic studies are necessary to determine how these two proteins interact and aggravate both pancreatic and brain pathologies.

Table of Contents

List of Figures

Abbreviations

Aβ – Amyloid-Beta

AD – Alzheimer's disease

ADDLs – Amyloid-Beta Derived Diffusible Ligands

AGEs – Advance Glycation End Products

Akt – Protein Kinase B

ALS – Amyotrophic Lateral Sclerosis

APP – Amyloid Precursor Protein

ApoE – Apolipoprotein E

β-cell – Beta Cell

BACE1 – Beta-secretase 1

BBB - Blood-brain barrier

BCA – Bichinchoninic Acid Assay

BGLs – Blood Glucose Levels

C99 – C-terminal 99-amino acid fragment

CSF – Cerebrospinal Fluid

DTg – Double Transgenic

EDTA - Ethylenediaminetertraacetic acid

ELISA - Enzyme-linked immunosorbent assay

FTD – Frontotemporal Dementia

Het – Heterozygous

huIAPP – Human Islet Amyloid Polypeptide or Amylin

IAPP – Islet Amyloid Polypeptide or Amylin

IHC – Immunohistochemistry

I.C. – Intra-cerebral

I.P. – Intra-peritoneal

LTP – Long Term Potentiation

MCI - Mild cognitive impairment

NFTs – Neurofibrillary Tangles

PAM – Peptidylglycine Alpha-Amidating Monooxygenase

PD – Parkinson's disease

PMDs – Protein Misfolding Disorders

ProIAPP – Proislet Amyloid Polypeptide

PC1/3 – Proprotein Convertase 1/3

PC2 – Proprotein Convertase 2

PrPSc - Misfolded prion protein

PS1 – Presenilin 1

PS2 – Presenilin 2

RT-PCR – Real Time-Polymerase Chain Reaction

S.E.M. - Standard Error of the Mean

ThT – Thioflavin T

TEM – Transmission Electron Microscopy

TSEs – Transmissible Spongiform Encephalopathies

T1D – Type I Diabetes

T2D – Type II Diabetes

CHAPTER 1

Introduction

Type II Diabetes and Alzheimer's disease Prevalence and Characteristics.

As the life expectancy of the population increases, as well as individuals living unhealthy lifestyles so too does the prevalence of age-related diseases such as Type II Diabetes (T2D) and Alzheimer's disease (AD). It is estimated that 25.8 million American individuals have diabetes – 90-95% being T2D (1). In addition, the total projected cost of diabetes in 2007 was 218 billion dollars (1). It is expected that 5.4 million individuals currently live with AD; moreover, the socioeconomic burden is tremendous costing $200 billion dollars (2). In addition, both diseases present complications to effectively diagnose individuals in that nothing is really offered for AD, as well as there are T2D affected individuals that go undiagnosed. By 2050, it is projected that the prevalence of diabetes and AD will double or even triple (1-2). Though these statistics are malicious enough already, recent research posits that having T2D can 2-5 fold increase the risk of AD (3-6); moreover, the number of T2D among AD patients is significantly augmented in comparison to age-matched non-AD controls (4, 7-8).

Type II Diabetes involves the dysfunctional use of pancreatic insulin by the body resulting in insulin resistance, hyperglycemia, hyperinsulinemia, pancreatic β-cell death, and other complications. Some of these diabetic complications can ultimately lead to cardiovascular disease, kidney disease, neuropathy, and diabetic retinopathy (9-10). Unlike Type I Diabetes (T1D), insulin is produced, but the body does not use it effectively. Insulin is an important hormone, and if the availability is insufficient, insulin is faulty, or the cell's response is defective (referring to sensitivity), then glucose will not be absorbed or stored properly by the cells. Thus, the net effect is high blood

glucose levels, irregular protein synthesis, and a number of other metabolic derangements. Intriguingly, in up to 96% of T2D patients, is the aggregation of an amyloidogenic species called islet amyloid polypeptide (IAPP) (3-7, 11) which is thought to have deleterious effects to the β-cells (12), yet it is unknown if IAPP is either a cause or an effect of the disease (13).

Characterized by Alois Alzheimer around 1905 from a patient named Auguste Deter, Alzheimer's disease is an age-related, chronic and progressive dementia characterized by extracellular amyloid-beta (Aβ) plaques, intracellular neurofibrillary tangles (NFTs), neuronal loss, brain inflammation, and cognitive impairment. Some of the known risk factors include: age (affecting 65 and up), the female gender, the APOE allele, and oxidative stress (2, 14). There is currently no definitive test (other than at autopsy) to diagnose AD, and there is no disease-modifying cure. Nowadays, the only treatment option is to slow the disease progression and manage the symptoms to ease the individual's life. More than 95% of the cases are considered sporadic, and inherited cases with genetic mutations in APP, PS1, and PS2 are less than 5% (2, 10).

Numerous studies have proposed diverse explanations for the interaction between these maladies such as defects in insulin signaling, anomalous glucose metabolism, formation of advanced glycation end products (AGEs), oxidative stress, activation of inflammatory pathways, other dysregulations of cellular processes (8, 10, 14-15), and, importantly for this study, abnormal protein processing. One of the important common features between T2D and AD is the presence of misfolded protein aggregates, which in the case of T2D consist of the accumulation in pancreas of islet amyloid polypeptide – (IAPP) and in AD brain (amyloid-beta - Aβ) (Fig.1) (16-17).

Nonetheless, T2D and AD are regarded as protein misfolding disorders (PMDs) due to their ability of amyloidogenesis. There are 20 more noted PMDs including Parkinson's disease (PD), Prion diseases, Huntington's disease (HD), Amyotrophic Lateral Sclerosis (ALS), among others.

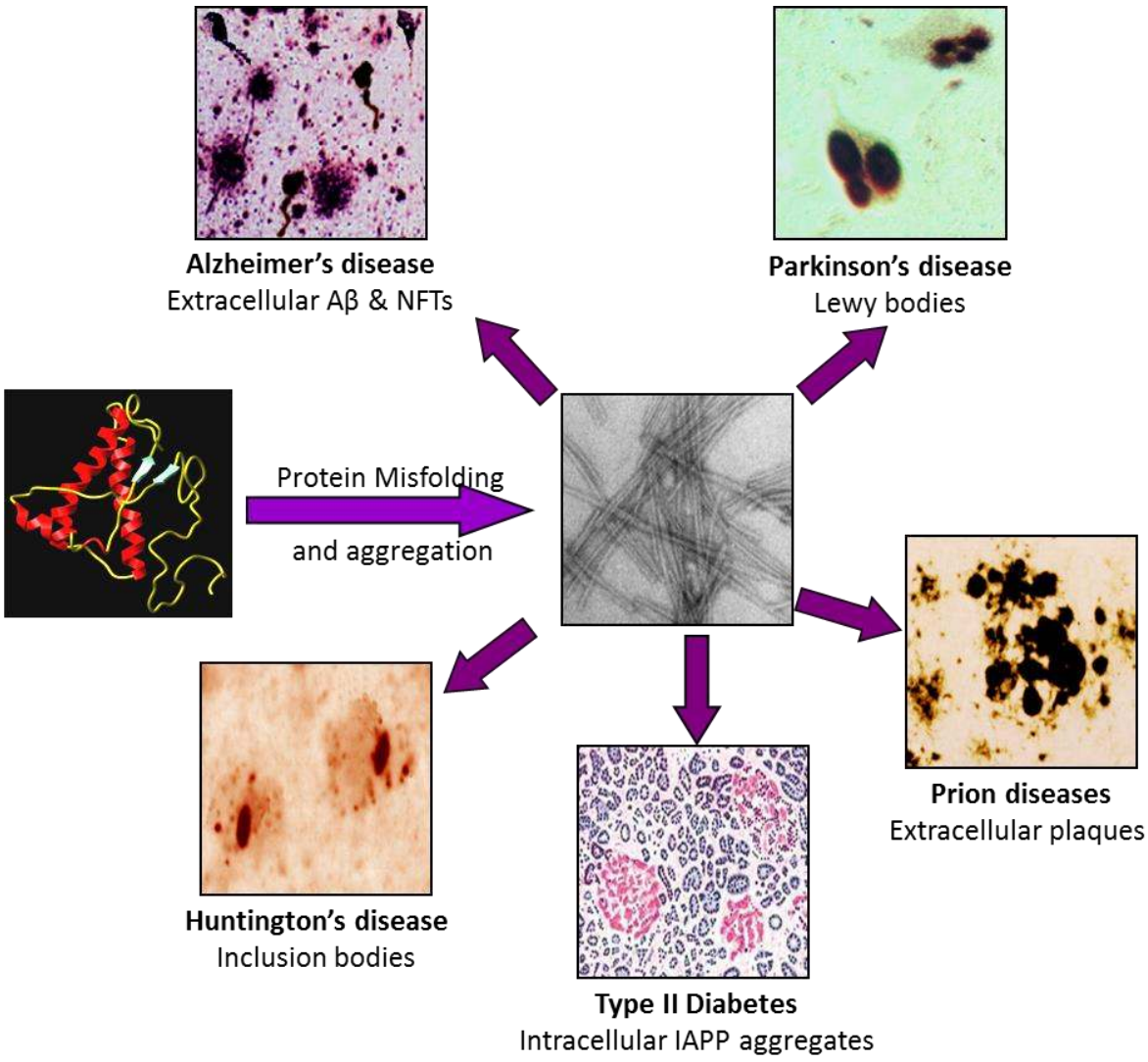

Figure 1. Protein Misfolding Disorders.

There are more than 20 diseases that are regarded as PMDs including: Prion diseases, Amyotrophic Lateral Sclerosis (ALS), Huntington's disease (HD), Parkinson's disease (PD), among others. T2D and AD are regarded as PMDs due to the presence of misfolded protein aggregates in pancreas (islet amyloid polypeptide - IAPP) for T2D and in brain (amyloid - Aβ) for AD affected individuals. Adapted by permission from Macmillan Publishers Ltd modified from Nature Reviews (16), copyright (2003).

Misfolded Protein Aggregates in Type II Diabetes and Alzheimer's disease.

Islet amyloid polypeptide (IAPP) or amylin is a hydrophobic 37 amino acid peptide hormone that is secreted from the β-cells in the pancreatic islets of Langerhans. The islets of Langerhans function to control blood sugar levels and glucose metabolism throughout the body by secretion of several substances such as glucagon, insulin, somatostatin, and amylin. Glucagon is secreted in response to low blood sugar levels, and it stimulates the liver to convert glycogen into glucose. Insulin is secreted in response to high blood glucose levels, and it also regulates the usage of glucose - whether it enters the cells for energy or goes back to the liver for storage. Insulin is an important hormone and has multiple functions throughout the body. In the brain, studies have shown insulin to regulate neuronal survival, energy metabolism, plasticity of neurons, and growth factors (18-19). In addition, it plays a role in learning and memory (14, 19). Somatostatin is located in the delta cells of the islet of Langerhans and is known to suppress the release of gastrointestinal hormones, inhibiting the release of insulin and glucagon.

IAPP is released as proislet amyloid polypeptide (proIAPP) and depends on blood glucose level (BGL) machinery (20-21) (Fig 2.). IAPP is co-secreted with insulin (1:100) from the pancreatic β-cells making insulin far more abundant. IAPP function is somewhat unclear, yet it is thought to contribute to glycemic control and is an inhibitor of the appearance of nutrients (especially glucose) in the plasma by delaying gastric emptying, inhibiting digestive secretion, and overall reducing food intake (giving a satiated feeling) (21); thus, IAPP is originated in the pancreatic β-cells and circulated through the blood crossing the blood-brain barrier (BBB) (21-22). IAPP has also been

assumed to have a role in the progression of insulin resistance in T2D patients (22). IAPP has been described to regulate bone metabolism and, though controversial, as an inhibitor of insulin, under certain conditions (22-24). As for regulation, little is known about the regulation of amylin synthesis, yet it is assumed since it has a close link to insulin being co-stored and co-secreted that it may follow the same regulatory mechanisms of insulin (21). Once IAPP is aggregated as a pancreatic amyloid, it is proposed that it contributes to the advancing decline of β-cell number and mass as well as later the problems with insulin secretion (4, 6, 12, 25). As previously stated, autopsy reports indicate that up to 96% of T2D patients have pancreatic IAPP aggregation (7, 9); besides humans, cats and macaques can develop T2D, and time-course studies in these animals showed that the accumulation of IAPP aggregates in the pancreas precede the symptoms of diabetes (20).

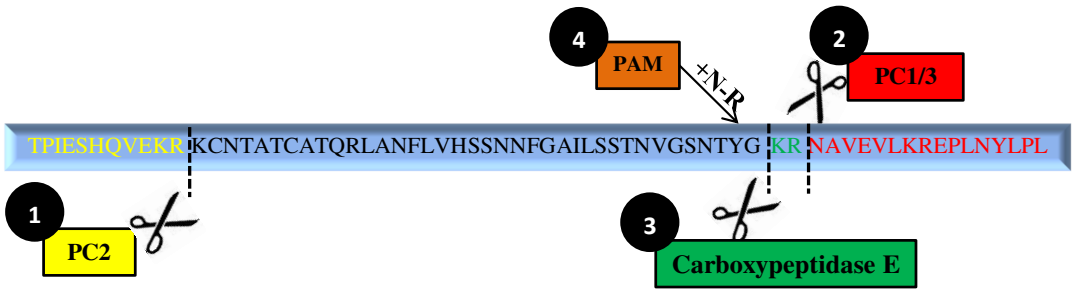

Figure 2. IAPP Processing. IAPP is processed from an 89-residue coding sequence (proIAPP) that is produced in pancreatic β-cells as a 67 amino acid: (1) 11 amino acids are removed from the N-terminal by enzyme proprotein convertase 2 (PC2); (2) 16 amino acids are removed from the C-terminal by proprotein convertase 1/3 (PC1/3); (3) at the C-terminus carboxypeptidase E removes the lysine and arginine residues; (4) peptidylglycine alpha-amidating monooxygenase (PAM) adds an amine group at the C-terminal glycine.

The main component of Aβ plaques, a typical hallmark of AD, is a 39-43 amino acid polypeptide engendered by an alternative proteolytic cleavage of amyloid precursor protein (APP) by β-secretase 1 (BACE1) and γ-secretase leading to the formation of neurotoxic species (Fig. 3). Alpha secretase cleaves the ectodomain at a closer site of the transmembrane domain of APP producing a non-amyloidogenic, easily-cleared peptide known as P3; besides, BACE1 cleaves within the ectodomain producing a C-terminal fragment substrate for γ-secretase that becomes the amyloidogenic Aβ (8, 16). The most deleterious Aβ form proposed is Aβ-42, but the most abundant form is Aβ-40. During many years, researchers focused on the insoluble Aβ fibril deposits as the leading cause of memory loss and neurodegeneration in AD, yet recent work has shown that the soluble oligomers may be the most toxic species (especially in the early stages),

which cause neuronal death and inhibit long term potentiation (LTP) (16-17, 26-29). Aβ has an unknown function, but in healthy individuals it is easily cleared from the brain unlike in AD affected individuals. Another hallmark of AD is the production of NFTs from hyperphosphorylated tau, which is a soluble microtubule associated protein localized within the axons and expressed in mature neurons; Aβ is known to interact with signaling pathways that control tau phosphorylation (2, 8, 14, 27).

Both IAPP and Aβ can misfold and aggregate forming large and insoluble deposits known as amyloid. The amyloid structures have a β-sheet conformation that is detected by Congo Red and Thioflavin dyes, have a characteristic X-ray diffraction pattern, and are highly resistant to proteolytic degradation (16, 21, 27). Immunopositive ubiquitin staining can normally be detected in amyloid aggregates due to a failed attempt by the proteasome to try to clear these deleterious aggregates, which suggests the high resistance to proteolytic degradation of the amyloid fibrils due to their complex structure, being too large to fit into the protein degrading machinery, and their insolubility (8). IAPP and Aβ fibril-like structures also can be recognized by transmission electron microscopy (TEM).

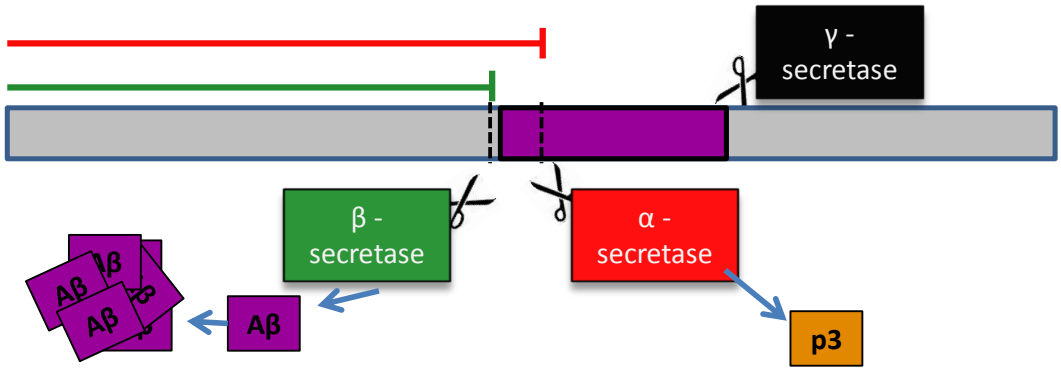

Figure 3. Formation of Aβ through APP Cleavage. Beta secretase (BACE1) is a transmembrane aspartyl protease that cleaves within the ectodomain of APP, leaving the C-terminal 99-amino acid fragment (C99) containing the single transmembrane domain, and becomes a substrate for the γ-secretase. Thus, the γ-secretase cleaves C99 at a variable location creating an amyloidogenic protein (Aβ-40, Aβ-42) to be released to the extracellular environment. Alpha secretase cleaves the ectodomain at a closer site of the transmembrane domain of APP and also creates a substrate for γ-secretase producing a non-amyloidogenic, easily-cleared peptide known as P3.

IAPP and Aβ share several characteristics, including they are both amyloidogenic, show 38% sequence similarity (6, 30), are directly toxic (6, 22), can activate proinflammatory responses as well as downstream pathways, and can alter Ca^{2+} homeostasis by affecting downstream pathways causing cell death (31). Aβ and IAPP are present in blood serum and cerebrospinal fluid (CSF) (30). Potential proof of hetero-association between Aβ and IAPP was seen when hot spot regions were identified in

these amyloids causing a propensity of Aβ and IAPP to interact. The results of this study showed that IAPP [8-18] and IAPP [22-28] sequences are hot regions of the IAPP and Aβ-40 interaction, and Aβ [27-32] and Aβ [35-40] were identified as the shortest sequences that were able to bind to IAPP with nanomolar affinity (Figure 4) (30). IAPP's toxic nature was modeled by synthetic human IAPP aggregates that are able to induce β-cell apoptosis (12); in addition, the inhibition of IAPP accumulation or synthesis results in the improvement of β-cell life in a human islet culture model (12, 25) – similarly this is noted with *in vitro* experiments using Aβ as well (17, 26).

Figure 4. Comparison of Sequences of Aβ and IAPP. In blue are the identical amino acids with similar residues in green. The shortest sequences with highest similarity are underlined in yellow. Sequences that are thought to play a role in self-association are underlined in pink. Image taken from Andreetto E. et. al. 2010

The Seeding-Nucleation and Cross-Seeding Model.

In amyloid formation it is noted the non-toxic, soluble, natively folded protein undergoes a conformational transition into a toxic, insoluble, and β-sheet comprising aggregate (32). The accumulation of misfolded aggregates (i.e. IAPP, Aβ) is thought to

follow a seeding-nucleation model in which a small and soluble misfolded oligomer (can range from dimers to decamers) acts as a nucleus to propagate misfolding by recruiting the native proteins into polymers (13, 16-17, 27, 33-36). In this model seen in Figure 5, misfolded "seeds" are produced during a nucleation or lag phase – a thermodynamically unfavorable stage where the folded protein changes its conformation to form a misfolded intermediate. The misfolded intermediate is highly unstable, but can be stabilized by oligomerization. When the misfolded oligomers are stable enough to resist clearance, the polymerization or exponential phase occurs where the oligomers rapidly and exponentially enlist native proteins to misfold. As a result of these aberrant interactions, protein aggregates have a proclivity to form large aggregates, become insoluble, and resistant to proteolysis, thus impervious to cellular clearance. Since the limiting step in this process is the formation of misfolded oligomeric seeds, the introduction of a pre-formed "seed" can accelerate the reaction by attenuating the nucleation phase (Fig. 5) (17, 33). Cross-seeding occurs when oligomers composed by one protein seed the aggregation of a different protein (16, 33). This heterologous cross-seeding has been demonstrated *in vitro* and *in vivo* involving several misfolded aggregates by interactions including the prion protein PrP^{Sc} and Aβ (37), Aβ and α-synuclein (38-40), Aβ and tau (35, 41-42), and others.

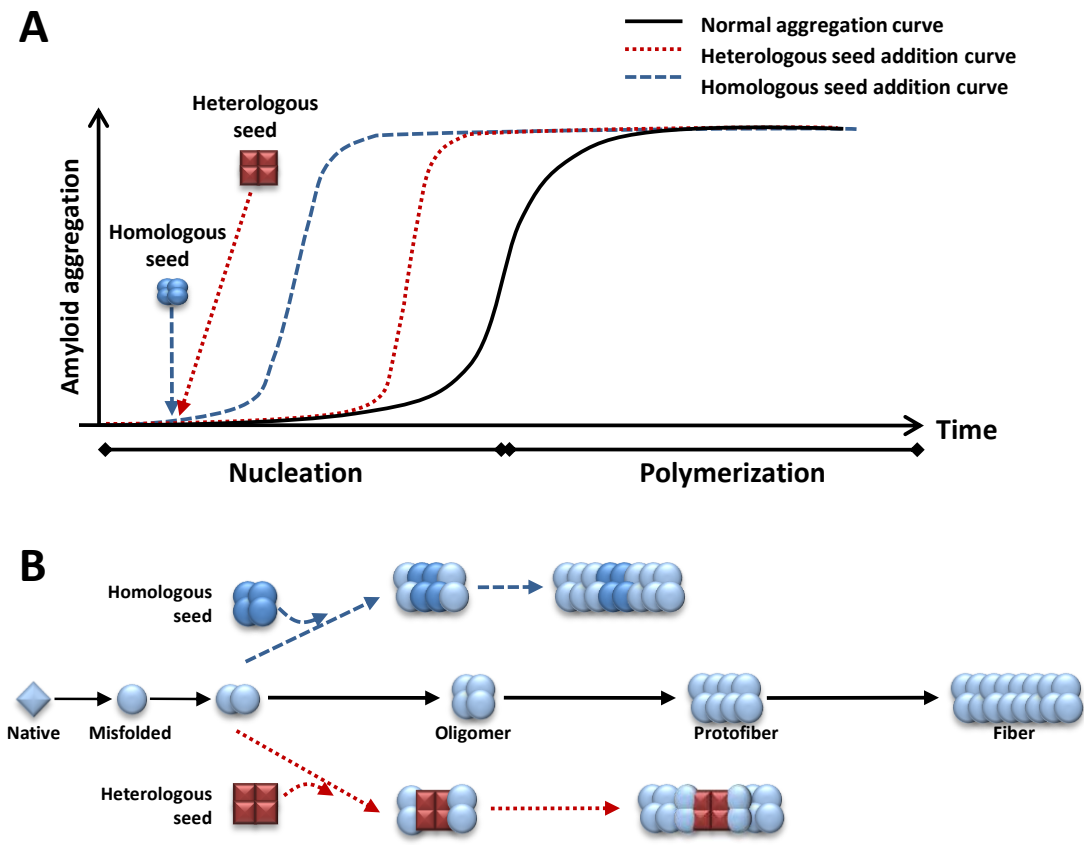

Figure 5. The Cross-Seeding Model. A) The misfolding and aggregation of proteins follows a seeding-nucleation model in which the key event is the formation of misfolded oligomeric seeds during the nucleation phase that acts as a scaffold building up aggregation and forming the oligomeric and fibril species. Thus, the seed formed in this nucleation or lag phase shortens the lag phase, and then after in the polymerization phase, the seeds quickly and exponentially enlist inherent proteins. Moreover, protein aggregation can be accelerated by the addition of preformed seeds. B) In some cases, the seed can originate from a different misfolded protein, which can cross-seed the process of protein misfolding and aggregation. Whether it is a homologous or heterologous seeding, the nucleation phase is shortened leading to an acceleration of protein aggregation.

Hypothesis

Our hypothesis is that the high coexistence of Type II diabetes and Alzheimer's disease may in part be due to cross-seeding of islet amyloid polypeptide and amyloid beta. In this Master Thesis project, we have studied this possibility *in vitro* and *in vivo* in a mouse model that has been engineered to develop both IAPP and Aβ aggregates and analyze whether the addition of IAPP or Aβ "seeds" exacerbates the disease pathology of T2D and AD through pathological, immunohistochemical, and biochemical analysis.

The research presented in this dissertation is analyzing this cross-seeding hypothesis as a potential molecular explanation for the synergism known between T2D and AD. We believe that an enhancement in disease pathology could be due to a cross-seeding effect between IAPP and Aβ and could elucidate the high co-existence of T2D and AD cases seen in human patients. Therefore, we will study the relationship of the protein aggregates IAPP and Aβ and their effect on these maladies by the following aims:

1) Analyze cross-seeding interaction between Aβ and IAPP utilizing *in vitro* studies
2) Determine the influence of Aβ aggregated "seeds" on T2D pathology in a double transgenic mouse model
3) Evaluate the influence of IAPP aggregated "seeds" on AD pathology in a double transgenic mouse model

CHAPTER 2

Analyze cross-seeding interaction between Aβ and IAPP utilizing *in vitro* studies

Rationale

The seeding-nucleation model states that protein misfolding and aggregation is a nucleation-dependent phenomenon in which a misfolded intermediate is formed during the lag phase and once a critical amount of these nuclei are created, the exponential phase starts, where the oligomeric species grow and extend producing fibrils. This model also states that the introduction of a preformed seed in the system is able to induce and accelerate protein aggregation, thus attenuating the nucleation or lag phase in the aggregation curve reaching the polymerization phase at a quicker rate. This can occur when the nuclei are of the same nature referring to homologous seeding, which shortens the nucleation phase. Cross-seeding or heterologous seeding occurs when the seeds of one particular protein accelerate the misfolding of a second particular protein. The resulting oligomers and fibrils will be composed by a combination of both proteins. Previous work has demonstrated this cross-seeding hypothesis *in vitro* and *in vivo* involving misfolded aggregates including the misfolded prion protein PrP^{Sc} and Aβ (37), Aβ and α-synuclein (38-40), Aβ and tau (35, 41-42), and others. The goal of this aim is to emulate the potential cross-seeding between Aβ and IAPP within the test tube. Seeding kinetic experiments will occur utilizing synthetic peptides (Aβ or IAPP) that will be incubated with the opposing aggregate form (so called seeds) at various concentrations (i.e. synthetic IAPP with purified Aβ aggregates and vice versa). Thioflavin T assay will be used as a method to specifically monitor the formation of amyloid aggregates. The ThT fluorescence originates from the dye reacting to amyloid fibrils (43). We expect that these *in vitro* studies will show cross-seeding of IAPP misfolding and aggregation induced by Aβ aggregates and that Aβ misfolding and

aggregation induced by IAPP aggregates is accelerated. We anticipate the seeds will shorten the nucleation or lag phase for polymerization.

Results

After running Bichinchoninic acid (BCA) assay to quantify the protein concentration of each IAPP and Aβ synthetic peptide and running an aggregation assay to check the viability of seed-free material, we began running the homologous and heterologous seeding for each specific protein.

In vitro IAPP Heterologous Cross-Seeding Accelerates Aβ aggregation.

With IAPP and Aβ having such close sequence similarities, as well as being amyloidogenic, IAPP oligomeric species were used to analyze whether Aβ misfolding and aggregation would be accelerated due to addition of these seeds. It would be essential to see both homologous and heterologous seeding occur at a faster rate than the standard set seeding curve for Aβ by a shortening of the nucleation or lag phase. Utilizing the ThT assay, briefly, 10% of IAPP oligomer seeds (heterologous seeding) or 10% Aβ oligomer seeds (homologous seeding) along with the monomeric Aβ-42 seed-free was added to a 96 well plate; the control was an insertion of the buffer the oligomer was originated. The percentage of seeds corresponds to the monomeric seed-free added per well. The fluorescence was read by a fluorometer at excitation 435 and emission 485 nm with intensity over time.

First, we needed to illustrate that Aβ misfolding and aggregation is, as previously described, induced by homologous Aβ oligomers. In Figure 6, the results demonstrate a speeding up of Aβ aggregation by the shortening of the lag phase due to the introduction of homologous seeds compared to the control. Regarding homologous seeding there is an acceleration of Aβ fibrillogenesis shown by the 10% homologous Aβ

seeding reaching 100% aggregation at about 40 hours faster than the control, respectively. These results corroborate the fact that Aβ misfolding was accelerated by the addition of homologous Aβ seeds by attenuation of the nucleation/lag phase accelerating Aβ misfolding and aggregation.

The results illustrate that the heterologous seeding of IAPP was able to reduce the lag phase. Figure 6 displays the heterologous seeding where there is an acceleration of Aβ aggregation and polymerization due to IAPP oligomeric seeds - 10% heterologous IAPP seeding reached 100% aggregation at about 25 hours, 10% homologous Aβ seeding reached 100% aggregation at about 40 hours, and the control reached 100% aggregation at about 72 hours, respectively. Both seeding curves were statistically significant from the control seeding curve. A reason that the heterologous IAPP seeding aggregated earlier than the homologous could be due to the higher amyloidogenicity of IAPP compared to Aβ allowing misfolding and accumulation to occur at a faster pace (44-47); in addition, the heterologous IAPP seeding could present more available oligomeric and/or fibrillogenic species for a faster reaction. The results elucidate that IAPP is an effective, viable seed for Aβ-42 aggregation by decreasing the lag phase for Aβ misfolding and aggregation and, thereby, inducing a faster Aβ aggregation. As expected, there is a cross-seeding effect in Aβ aggregation in the presence of IAPP oligomers.

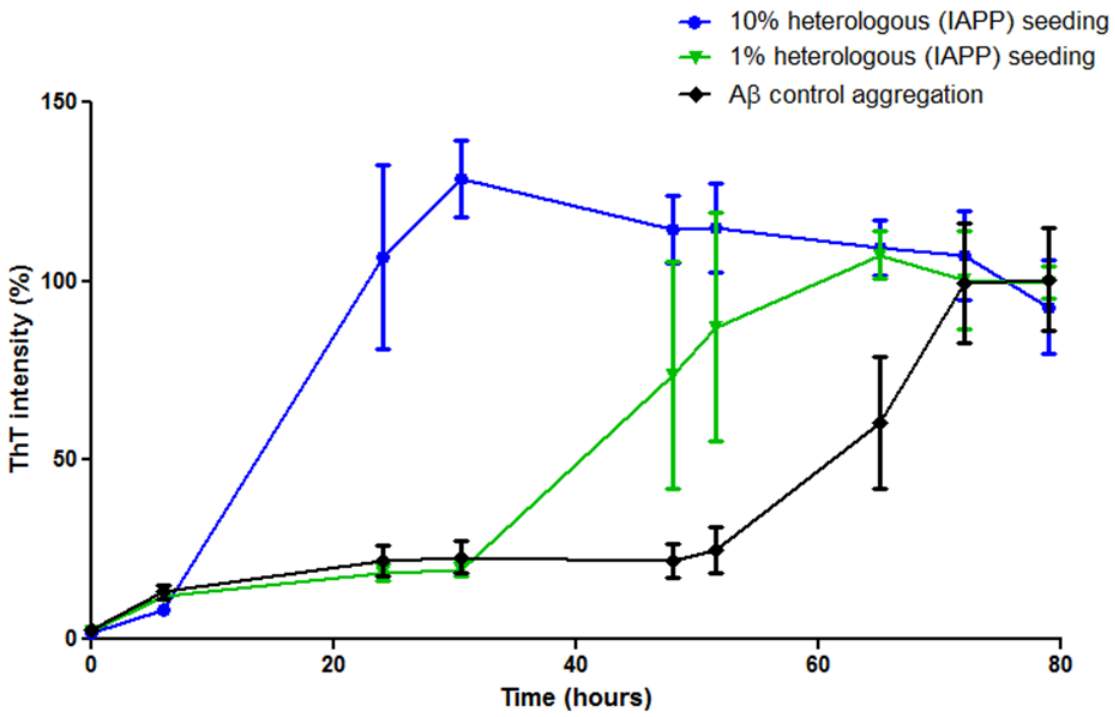

Figure 6. *In vitro* Aβ Aggregation is Enhanced by Adding Heterologous IAPP Seeds. Aβ misfolding and accumulation is expedited by the addition of 10% heterologous IAPP seed or 10% homologous Aβ seed that causes the nucleation phase to diminish. Statistical analysis: Two-way ANOVA; p value < 0.0001; p value = 0.0065.

Aβ Heterologous Cross-Seeding Increases IAPP aggregation *In vitro*.

Aβ-42 oligomeric seeds were used to test whether IAPP misfolding and aggregation would be accelerated. It would be essential to see both homologous and heterologous seeding occur at a faster rate than the standard set seeding curve for IAPP by an attenuation of the nucleation or lag phase. To analyze cross-seeding, ThT Assay was performed by adding 1% homologous IAPP oligomeric seeds or 1% heterologous Aβ oligomeric seeds, and the fluorescence read by a fluorometer at excitation 435 and emission 485 nm with intensity over time. One major deterrent in which several studies

have noted is that IAPP can essentially have a very short or even no lag phase upon incubation at a neutral pH, even more so with the addition of homologous seeds (44-47). In order to confirm IAPP seeding *in vitro*, we needed to exemplify that IAPP misfolding and aggregation would be accelerated by adding homologous IAPP oligomers. Our results show that the homologous IAPP aggregate was able to speed up IAPP misfolding and aggregation, as reported before (34, 44-45, 48). Figure 7 demonstrates an acceleration of IAPP fibrillogenesis due to the concentration of homologous IAPP oligomeric seeds with the 1% IAPP oligomer seeding curve reaching 100% aggregation at about 1 hour. This evidence elucidates that IAPP does follow the seeding-nucleation model; IAPP aggregates are able to decline the nucleation phase, thus accelerating IAPP misfolding and aggregation. Following the same procedure as above, 1% heterologous Aβ oligomeric seeds were added to accelerate the aggregation reaction of IAPP. The results show that the heterologous seeding with Aβ was able to shorten the lag phase accelerating IAPP aggregation. Figure 7 exhibits both seedings of IAPP where there is an acceleration of IAPP aggregation due to heterologous or homologous seeds - 1% heterologous Aβ seeding reached 100% aggregation at about 4 hours, 1% homologous IAPP seeding reached 100% aggregation at about 1 hour, and the control reached 100% aggregation over 13 hours, respectively. Both seeding curves were statistically significant from the control seeding curve. We are able to confirm that the addition of a seed, whether IAPP or Aβ, that there is a very short lag phase, yet the standard IAPP control takes hours to elevate.

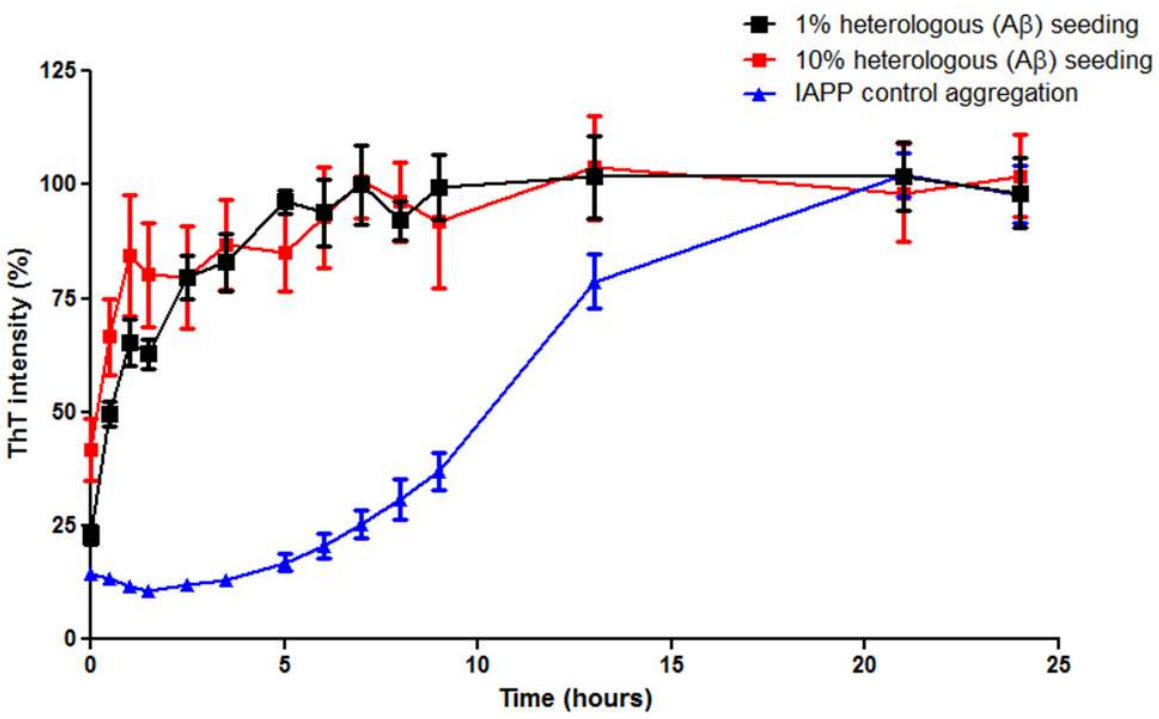

Figure 7. *In vitro* IAPP Aggregation is Enhanced by the Addition of Aβ Seeds.

The heterologous seeding with Aβ-42 was able to deplete the lag phase with acceleration of aggregation at with 1% oligomers. 1% heterologous Aβ seeding reached 100% aggregation at about 4 hours, 1% homologous IAPP seeding reached 100% aggregation at about 1 hour, and the control reached 100% aggregation at about 13 hours. Statistical analysis: Two-way ANOVA; p value < 0.0001.

Summary

In this section, we wanted to determine a cross-seeding interaction between IAPP and Aβ *in vitro*. This was done by utilizing the ThT assay incubating IAPP oligomeric species on synthetic Aβ-42 peptides and vice versa with different quantities (10 and 1%) to acquire a shortened nucleation phase from the standard seeding curve. Both heterologous seedings, IAPP oligomers into Aβ aggregation and Aβ oligomers into IAPP aggregation, demonstrated quicker kinetics by reacting to the auxiliary seed, by misfolding and aggregating at accelerated rates compared to the controls. Further work is necessary such as addition of controls - incubation with the opposing monomeric seed-free or incubation with a different proteins aggregate (i.e. albumin).

CHAPTER 3

Determine the influence of Aβ aggregated "seeds" on T2D pathology in a double transgenic mouse model

Rationale

After obtaining the DTg $IAPP^{+/+}/APP_{Swe}^{+/-}$ mice expressing both human IAPP and human Aβ and appropriate genotypic controls - heterozygous $IAPP^{+/-}/APP_{Swe}^{+/-}$, $huIAPP^{+/+}$, and $huIAPP^{+/-}$ on the double background- we assessed the effect of Aβ aggregates cross-seeding IAPP on T2D pathology (i.e. aggregation of IAPP in the pancreas) by analyzing the clinical symptoms and pancreatic histopathology of these animals. We plan to emulate what is found in affected individuals of these two PMDs – T2D and AD. A putative clinical symptom of T2D is hyperglycemia. We expect that the presence of Aβ oligomers will act as a seed increasing IAPP deposition in the β-cells. The augmentation of aggregated IAPP could induce β-cell death, decreasing insulin production and aggravating hyperglycemia in DTg animals in comparison with control animals. Moreover, we will analyze the difference of pancreatic amylin deposition in these mice by employing immunohistochemical measurements. We expect to observe augmented immunopositive IAPP accumulation in the pancreas as well as intensified BGLs in the DTg $IAPP^{+/+}/APP_{Swe}^{+/-}$ animals to support our cross-seeding hypothesis.

Results

DTg IAPP$^{+/+}$/APP$_{Swe}^{+/-}$ Demonstrate Accentuated Blood Glucose Levels (BGLs).

In order to analyze Aβ aggregates acting as a "seed" on T2D pathology as well as the interaction of these associated protein aggregates, we developed DTg IAPP$^{+/+}$/APP$_{Swe}^{+/-}$ mice that engender both IAPP and Aβ aggregates and analyzed BGLs. An anomalous increase of blood glucose levels is a common symptom of diabetes. The American Diabetes Association currently describes diabetes as having fasted blood glucose levels at >126 mg/dL, which is lower than the previous fasted glucose >140 mg/dL (10, 49). Mice showing hyperglycemia are regarded having a >150 mg/dL fasted blood glucose levels while normal mammals are said to be <110 mg/dL (50). To analyze the effect of the coexistence of both amyloidogenic proteins on hyperglycemia, we verified the BGLs of the animals by a tail vein nick using Contour blood glucose test strips (Bayer Healthcare) upon sacrificing the animals at about 250 days of age to analyze the auxiliary effect of Aβ on this typical clinical symptom seen in T2D. Figure 8 shows the DTg IAPP$^{+/+}$/APP$_{Swe}^{+/-}$ mice had an average BGL at 171.2 mg/dL, while the Het IAPP$^{+/-}$/APP$_{Swe}^{+/-}$ had an average of 134.27 mg/dL, IAPP$^{+/+}$ of 108.67 mg/dL, and IAPP$^{+/-}$ of 100.13 mg/dL. The DTg IAPP$^{+/+}$/APP$_{Swe}^{+/-}$ mice demonstrated significantly elevated BGLs in comparison to the control Het IAPP$^{+/-}$/APP$_{Swe}^{+/+}$, IAPP$^{+/+}$, and IAPP$^{+/-}$ as demonstrated by one-way ANOVA statistical analysis. The significant elevation in BGLs posits an exacerbation of hyperglycemia in animals harboring both Aβ and IAPP human proteins in comparison with animals that express just human IAPP.

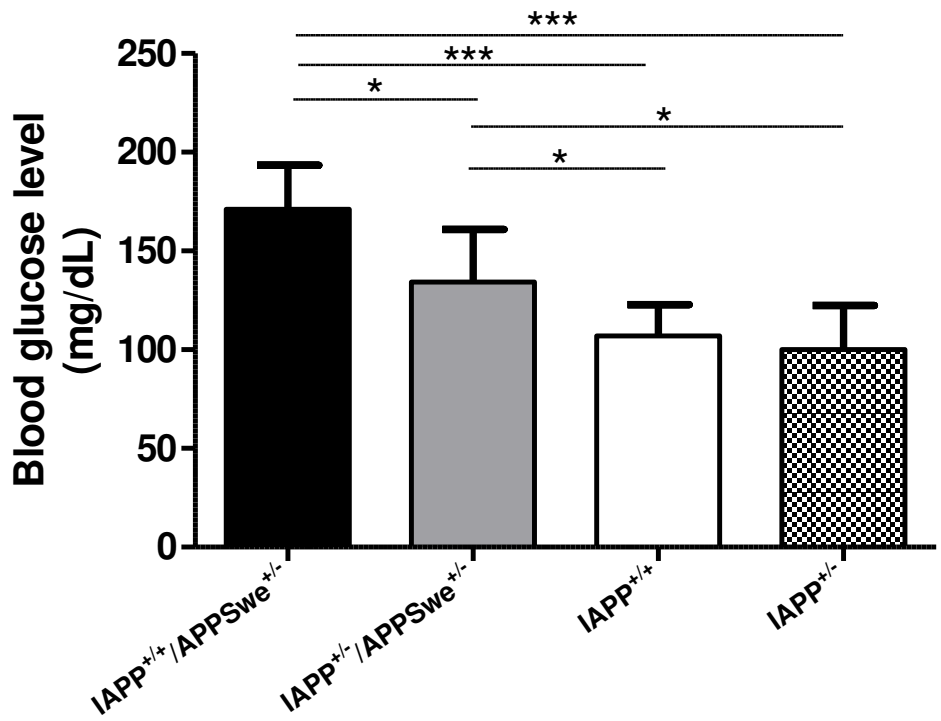

Figure 8. DTg IAPP$^{+/+}$/APPSwe$^{+/-}$ Demonstrate Significantly Elevated BGLs. One of the canonical T2D pathological traits is high blood glucose levels (BGLs). The auxiliary effect of Aβ on this typical T2D clinical symptom shows that the DTg IAPP$^{+/+}$/APPSwe$^{+/-}$ animals have higher BGLs than their appropriate genotypic controls. In addition, Het IAPP$^{+/-}$/APPSwe$^{+/-}$ have significantly higher BGLs than the IAPP$^{+/+}$ and IAPP$^{+/-}$. IAPP$^{+/+}$/APPSwe$^{+/-}$ mice show an exacerbation of hyperglycemia by displaying an increase of BGLs in comparison to their controls. Statistical analysis was done with GraphPad Prism 5.0; One-way ANOVA; Tukey's: *$p<0.05$; ***$p<0.001$

DTg IAPP$^{+/+}$/APP$_{Swe}^{+/-}$ Exhibit Elevated IAPP Burden Levels.

To analyze whether the presence of Aβ increases the deposition of IAPP in the pancreas, we quantified the amount of pancreatic IAPP through immunohistochemistry, using an antibody that recognizes the human sequence of IAPP. As shown in Figure 9, the DTg IAPP$^{+/+}$/APP$_{Swe}^{+/-}$ mice exhibit a higher amount of pancreatic IAPP staining than the controls - heterozygous IAPP$^{+/-}$/APP$_{Swe}^{+/-}$ and huIAPP$^{+/+}$. The DTg IAPP$^{+/+}$/APP$_{Swe}^{+/-}$ pancreas demonstrates an intense reactivity to the human amylin antibody compared to controls; in addition, the areas with more intense staining likely correspond to protein aggregates deposited in the tissue, although at this stage we cannot rule out that they represent higher production of the protein. Visually, it seems that the IAPP accumulation occurs intracellularly and then, once when there is a proliferation of misfolded protein, may expel out of the cell becoming extracellular due to cellular death (12-13). In addition, we quantified the IAPP pancreatic burden as seen in Figure 10. Intriguingly; we could see that the DTg IAPP$^{+/+}$/APP$_{Swe}^{+/-}$ mice exhibit a statistically significant increase of pancreatic amylin levels compared to their controls. The DTg IAPP$^{+/+}$/APP$_{Swe}^{+/-}$ had around a 1.1 fold augmentation in pancreatic IAPP levels compared to the Het IAPP$^{+/-}$/APP$_{Swe}^{+/-}$ as well as a 2.4 fold increase compared to the huIAPP$^{+/+}$. Further immunohistochemical analyses by double labeling the mouse pancreas utilizing a permutation of antibodies with IAPP and/or different antibodies used for islets (i.e. insulin) may give further information about the exact cellular location and colocalization of various proteins (7). Thus, with the additive effect of Aβ being introduced as a seed, the T2D characteristics of these mice seem to be aggravated compared to the age-matched controls.

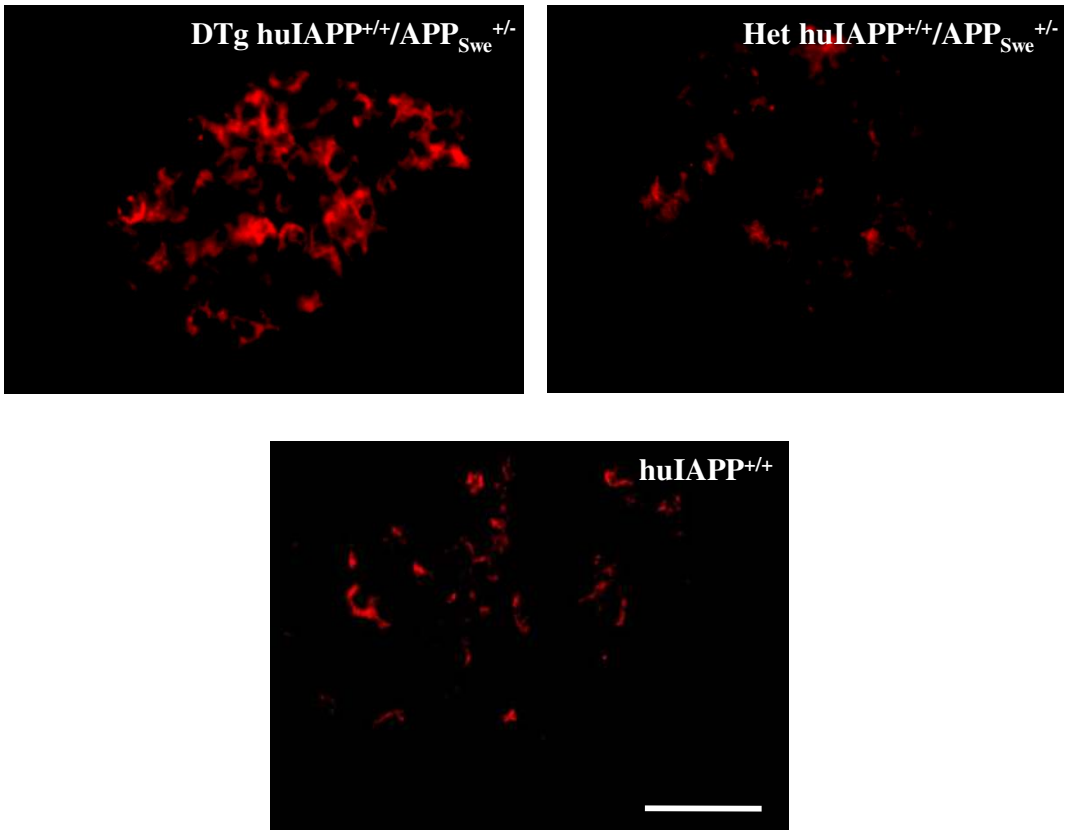

Figure 9. DTg IAPP$^{+/+}$/APP$_{Swe}^{+/-}$ Exhibit Elevated IAPP Burden Levels. Representative pictures of Langerhans islets IAPP immunostained in experimental and control animals. DTg IAPP$^{+/+}$/APPSwe$^{+/-}$ demonstrate augmented huIAPP pancreatic burden as seen by immunopositive reaction to anti-huIAPP antibody compared to their genotypic controls - heterozygous huIAPP/ APPSwe and huIAPP. Scale bar 100 um.

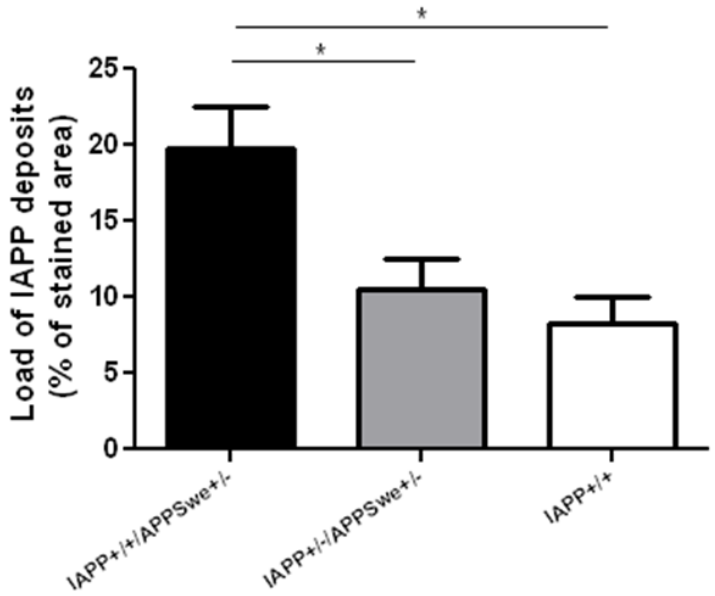

Figure 10. DTg IAPP$^{+/+}$/APPSwe$^{+/-}$ mice exhibit increased IAPP burden levels.

IAPP load was quantified by optical density in immunostained pictures by ImageJ software. Through quantification of pancreatic IAPP burden in these animals, DTg IAPP$^{+/+}$/APPSwe$^{+/-}$ mice show an increase of the load of IAPP aggregates in the pancreas in comparison to their controls. Statistical analysis: One-way ANOVA; Tukey's: *p<0.05

Heterozygous IAPP$^{+/-}$/APP$_{Swe}$$^{+/-}$ Mice Have T2D-like Pathology.

It is noted that even up to 2 years of age the regular heterozygous transgenic huIAPP mice have not been reported to develop any islet amyloid deposits nor any diabetic-like pathology, at any age (25, 51-54). However, in Figures 8 to 10, heterozygous IAPP$^{+/-}$/APP$_{Swe}$$^{+/-}$ have a diabetic-like phenotype at 20 weeks of age, even greater than that of the huIAPP$^{+/+}$ mice – significantly more elevated BGLs and high pancreatic IAPP levels, though not significant. Thus, the seeding presence of Aβ is seen to bring on T2D-like phenotype in these heterozygous IAPP$^{+/-}$/APP$_{Swe}$$^{+/-}$ which would

normally not be present in huIAPP$^{+/-}$ mice. To further verify these findings, the huIAPP+/- mice are planning to be immunohistochemically quantified. We expect that the huIAPP$^{+/-}$ animals will present lower amounts of pancreatic IAPP burden than the DTg IAPP$^{+/+}$/APP$_{Swe}$$^{+/-}$ and Het IAPP$^{+/-}$/APP$_{Swe}$$^{+/-}$ mice.

Summary

In this section, we investigated a T2D-like/AD mouse model, the DTg huIAPP$^{+/+}$/APP$_{Swe}^{+/-}$, that is able to generate both IAPP and Aβ emulating what is noted in human patients affected by the coexistence of these two diseases. Here, we wanted to determine the effect of Aβ seeds upon T2D pathology by analyzing the clinical (BGLs) and phenotypical (aggregation of IAPP) traits that are putatively recognized in T2D patients. The DTg huIAPP$^{+/+}$/APP$_{Swe}^{+/-}$ had augmented BGLs compared to the heterozygous huIAPP$^{+/-}$/APP$_{Swe}^{+/-}$ and huIAPP$^{+/+}$ mice, thus emphasizing an aggravation of this clinical symptom. The DTg huIAPP$^{+/+}$/APP$_{Swe}^{+/-}$ significantly displayed copious pancreatic IAPP burden levels in comparison to controls. Strikingly, the heterozygous huIAPP$^{+/-}$/APP$_{Swe}^{+/-}$ were able to show T2D-like pathology with elevated BGLs and pancreatic IAPP deposition, which is normally not plausible in the huIAPP$^{+/-}$ mice. Taken together, with the elevation of both BGLs and pancreatic IAPP burden levels, the presence of Aβ is seen to exacerbate T2D symptoms in the DTg huIAPP$^{+/+}$/APP$_{Swe}^{+/-}$ in comparison to the controls.

CHAPTER 4

Evaluate the influence of IAPP aggregate "seeds" on AD pathology in a double transgenic mouse model

Rationale

Utilizing the DTg $IAPP^{+/+}/APP_{Swe}^{+/-}$ mice expressing both human IAPP and human Aβ and appropriate genotypic controls - Het $IAPP^{+/-}/APP_{Swe}^{+/-}$, $APP_{Swe}^{+/-}$ injected with STZ (T1D control), and $APP_{Swe}^{+/-}$ on the double background - we assessed the effect of IAPP aggregates acting as a "seed" on AD pathology by analyzing accumulation of Aβ plaques in the brain of these animals. Analyzing immunohistochemically stained cortical and hippocampal slices, we expect that the co-expression of endogenous Aβ and IAPP will cause higher Aβ plaque burden and number of plaques per area in comparison to controls. We analyzed the hippocampus and cortex due to the extensive reports of AD pathology affecting these regions in the transgenic mice and human patients, as well as their role in learning and memory (16, 27). We expect to observe augmented immunopositive Aβ accumulation in the brain in the DTg $IAPP^{+/+}/APP_{Swe}^{+/-}$ animals, and a colocalization of both proteins in the brain to support our cross-seeding hypothesis.

Results

DTg IAPP$^{+/+}$/APP$_{Swe}^{+/-}$ Exhibit Increased Cortical and Hippocampal Aβ Burden Levels.

It has been established that IAPP secreted in the pancreas can cross the blood brain barrier and target different brain areas. We hypothesize that the presence of aggregated IAPP in the DTg animals will induce a higher aggregation and deposition of Aβ in the brain by a cross-seeding mechanism. The animals previously mentioned were studied to examine if there is an augmentation of AD pathology (cerebral and hippocampal Aβ plaques) due to the presence of IAPP aggregates. We expect to see an elevated Aβ plaque burden in these areas in the DTg IAPP$^{+/+}$/APP$_{Swe}^{+/-}$ animals to confirm acceleration in pathology in comparison to the Het IAPP$^{+/-}$/APP$_{Swe}^{+/-}$, APP$_{Swe}^{+/-}$ injected with streptozotocin (STZ) (T1D model), and APP$_{Swe}^{+/-}$.

Figure 11 displays representative images of the Aβ plaques reactive to 82E1 antibody (green). Visually we can see a difference in the size with the DTg IAPP$^{+/+}$/APP$_{Swe}^{+/-}$ in comparison to the Het IAPP$^{+/-}$/APP$_{Swe}^{+/-}$, APP$_{Swe}^{+/-}$ injected with STZ as T1D control, and APP$_{Swe}^{+/-}$. To prove that the augmented AD pathology is due to aggregated IAPP and not to the hyperglycemic environment or the reduction of insulin levels that also happen in the huIAPP animal model, STZ was injected into APP$_{Swe}^{+/-}$ acting as a T1D control. The diabetogenic drug STZ is known to be toxic to the β-cells when injected and ultimately destroys them; it is thought to work by having a similar glucose moiety that enables STZ to enter β-cells and causes toxicity by alkylation of DNA (55). We are seeing that the DTg IAPP$^{+/+}$/APP$_{Swe}^{+/-}$ animals have a more vigorous effect on AD pathology than STZ injected APP$_{Swe}^{+/-}$ animals.

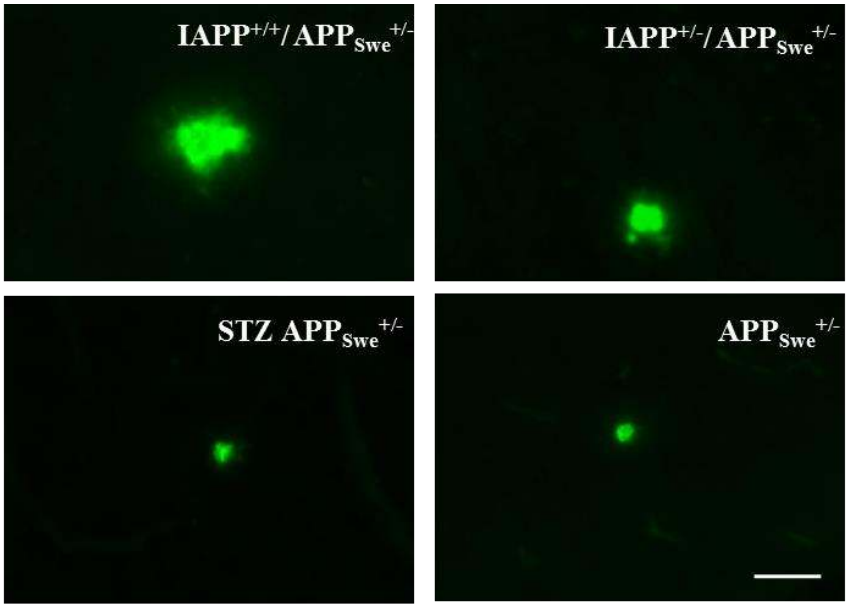

Figure 11. DTg IAPP$^{+/+}$/APP$_{Swe}^{+/-}$ Mice Display Higher Aβ Immunopositive Plaques in the Brain. Representative images of the cortex with amyloid plaques. Aβ aggregates are reactive to human anti-Aβ antibody 82E1 seen in fluorescent green. Larger and higher number of Aβ reactive plaques are seen in the DTg IAPP$^{+/+}$/APP$_{Swe}^{+/-}$ mice. Images were taken using epifluorescent microscope (DMI6000B, Leica) Scale bar: 50 um.

In addition, in Figure 12 cortical and hippocampal Aβ quantifications illustrate that the DTg $IAPP^{+/+}/APP_{Swe}^{+/-}$ have augmented Aβ burden in comparison to their genotypic controls. Moreover, the Het $IAPP^{+/-}/APP_{Swe}^{+/-}$ have greater cortical Aβ burden levels compared to the $APP_{Swe}^{+/-}$, representing a dose-dependence of the alleles. Cortical and hippocampal Aβ calculations were done by utilizing the percent of the area stained divided by the total area analyzed for Aβ load. Normally, the $APP_{Swe}^{+/-}$ or Tg2576 do not display AD-like pathology until a later age (56), yet the DTg $IAPP^{+/+}/APP_{Swe}^{+/-}$ are demonstrating this exacerbated pathology at 250 days of age; in addition, the larger plaques are displayed more in the DTg $IAPP^{+/+}/APP_{Swe}^{+/-}$ than any of the controls. Thus, these results indicate that the DTg $IAPP^{+/+}/APP_{Swe}^{+/-}$ have exacerbated AD pathology compared AD and AD/T1D transgenic animal models, suggesting that IAPP "seeds" bring elevated and earlier onset of Aβ burden in comparison to the controls.

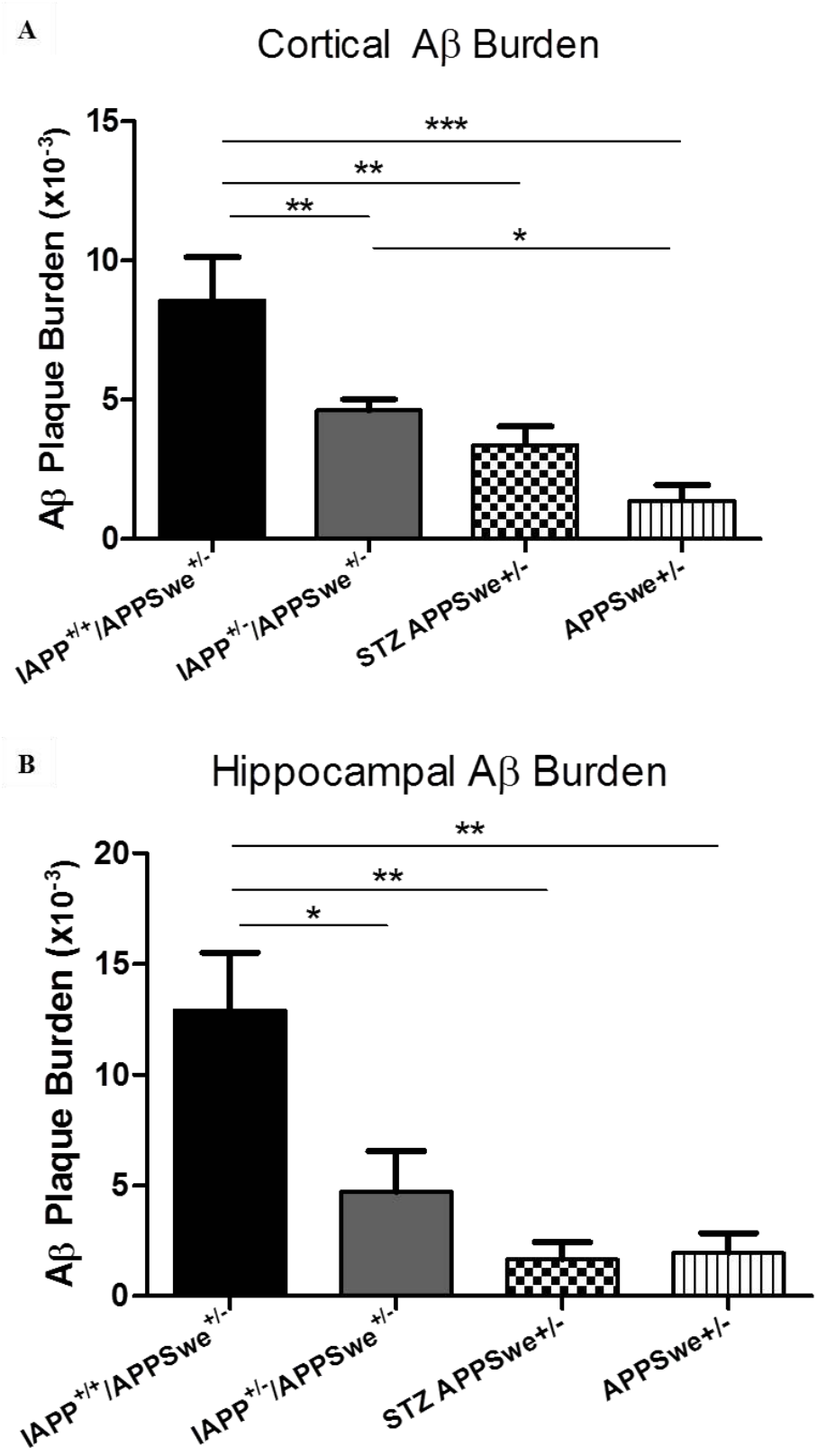
A
Cortical Aβ Burden
Aβ Plaque Burden (X10-3)
15
10
5
0
***
**
**
*
IAPP+/+/APPSwe+/-
IAPP+/-/APPSwe+/-
STZ APPSwe+/-
APPSwe+/-
B
Hippocampal Aβ Burden
Aβ Plaque Burden (X10-3)
20
15
10
5
0
**
**
*
IAPP+/+/APPSwe+/-
IAPP+/-/APPSwe+/-
STZ APPSwe+/-
APPSwe+/-

Figure 12. DTg IAPP$^{+/+}$/APP$_{Swe}^{+/-}$ Exhibit Increased Cortical and Hippocampal Aβ Burden Levels. (A) Quantification of Aβ burden shows DTg IAPP$^{+/+}$/APPSwe$^{+/-}$ mice have an exacerbated cortical Aβ burden compared to Het IAPP$^{+/-}$/APPSwe$^{+/-}$, APPSwe$^{+/-}$ injected with STZ as T1D control, and APPSwe$^{+/-}$. Heterozygous mice have an elevated cortical Aβ burden in comparison to APPSwe$^{+/-}$. Statistical analysis: One-way ANOVA; p value = <0.0001; Tukey's: *p<0.05; **p<0.01; ***p<0.001 (B) DTg IAPP$^{+/+}$/APPSwe$^{+/-}$ animals have an exacerbated hippocampal Aβ burden compared to Het IAPP$^{+/-}$/APPSwe$^{+/-}$, APPSwe$^{+/-}$ injected with STZ as T1D control, and APPSwe$^{+/}$. Statistical analysis: One-way ANOVA; ; p value = 0.0021; Tukey's: *p<0.05; **p<0.01.

DTg IAPP$^{+/+}$/APP$_{Swe}^{+/-}$ Reveal Increased Cortical and Hippocampal Aβ Density Levels.

As noted above, the DTg IAPP$^{+/+}$/APP$_{Swe}^{+/-}$, Het IAPP$^{+/-}$/APP$_{Swe}^{+/-}$, APP$_{Swe}^{+/-}$ injected with STZ, and APP$_{Swe}^{+/-}$ animal groups were assessed for Aβ plaques density. Density refers to number of plaques per mm^2 using scaled measurements in the brain. We expect to see an elevated Aβ plaque number in cortical and hippocampal areas in the DTg IAPP$^{+/+}$/APP$_{Swe}^{+/-}$ animals in comparison to control groups. Figure 13 displays the number of plaques per mm^2 in cortical with a difference in the DTg IAPP$^{+/+}$/APP$_{Swe}^{+/-}$ in comparison to all controls. Moreover, for cortical density the Het IAPP$^{+/-}$/APP$_{Swe}^{+/-}$ have greater Aβ density compared to the APP$_{Swe}^{+/-}$. This suggests that these animals demonstrate a dose-dependence of the alleles. Observing the hippocampal density, the DTg IAPP$^{+/+}$/APP$_{Swe}^{+/-}$ have more Aβ plaques per area in comparison to the APP$_{Swe}^{+/-}$

injected with STZ as T1D control and $APP_{Swe}^{+/-}$. The numbers of plaques in the DTg $IAPP^{+/+}/APP_{Swe}^{+/-}$ are elevated at earlier time indicating an acceleration of the AD pathology; thus, these results posit that the DTg $IAPP^{+/+}/APP_{Swe}^{+/-}$ once again have a more intensified AD pathology possibly due to the presence of IAPP "seeds".

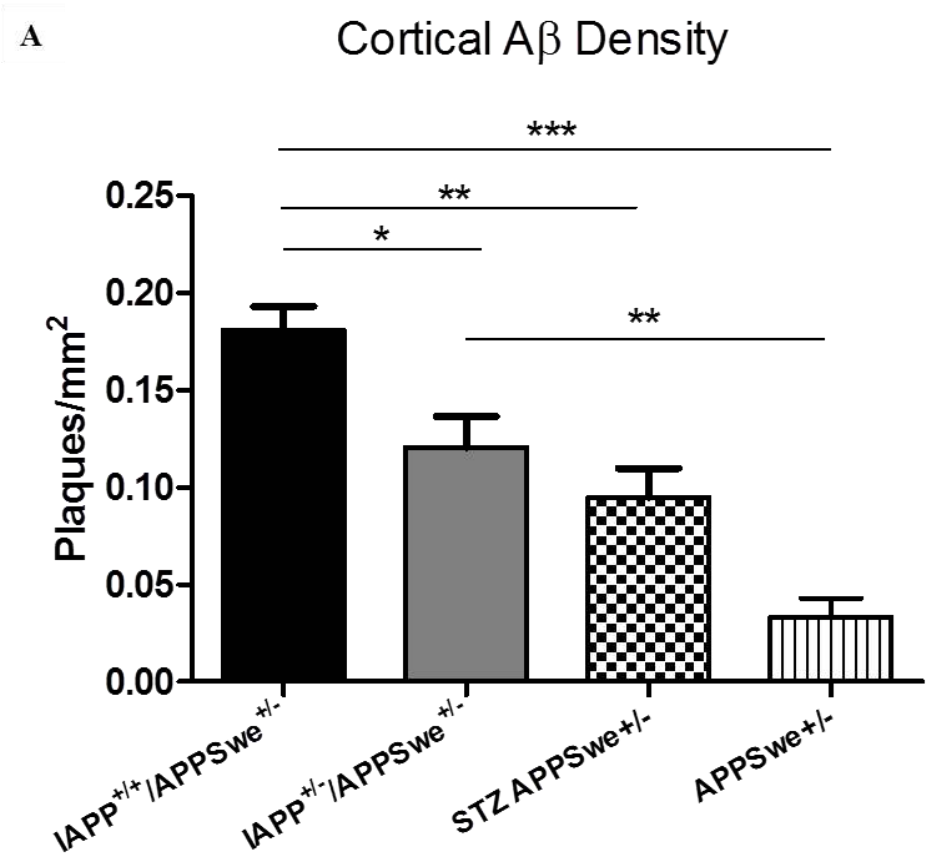
A
Cortical Aβ Density
***
**
*
**
0.25
0.20
0.15
0.10
0.05
0.00
Plaques/mm2
IAPP+/+/APPSwe+/-
IAPP+/-/APPSwe+/-
STZ APPSwe+/-
APPSwe+/-

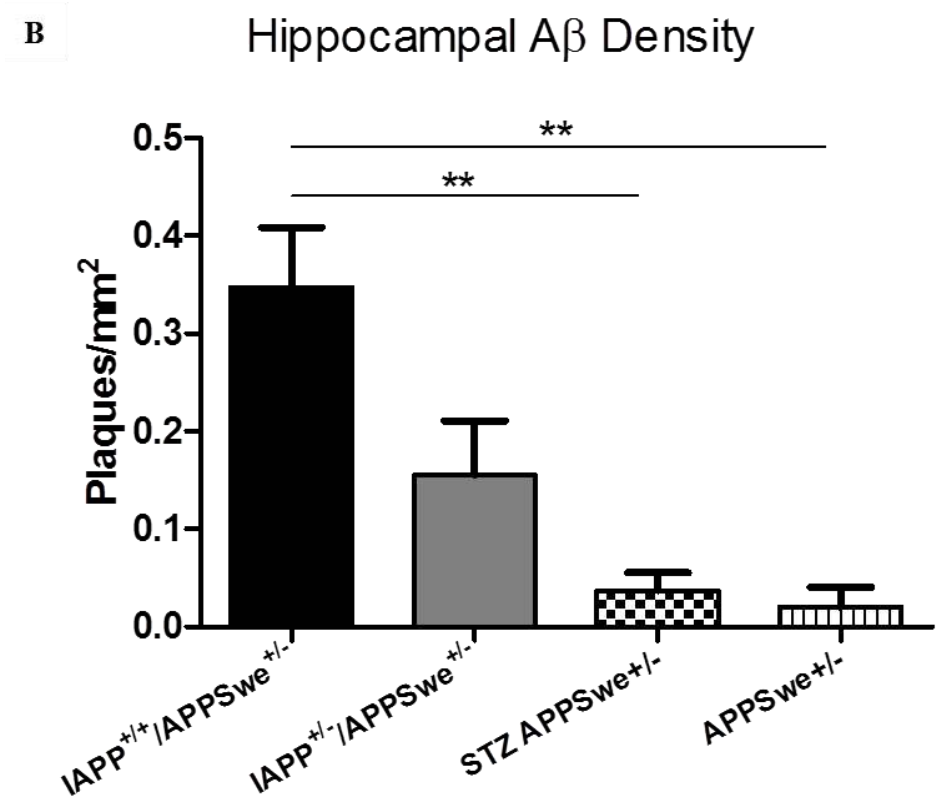
B
Hippocampal Aβ Density
**
**
0.5
0.4
0.3
0.2
0.1
0.0
Plaques/mm2
IAPP+/+/APPSwe+/-
IAPP+/-/APPSwe+/-
STZ APPSwe+/-
APPSwe+/-

Figure 13. DTg IAPP$^{+/+}$/APP$_{Swe}^{+/-}$ Reveal Increased Cortical and Hippocampal Aβ Density Levels. (A) DTg IAPP$^{+/+}$/APP$_{Swe}^{+/-}$ demonstrate augmented cortical Aβ density in comparison to controls STZ injected APP$_{Swe}^{+/-}$ (T1D control) and APP$_{Swe}^{+/-}$. Het IAPP$^{+/+}$/APP$_{Swe}^{+/-}$ mice have an elevated cortical Aβ density in comparison to APP$_{Swe}^{+/-}$. Statistical analysis: One-way ANOVA; p value < 0.0001; Tukey's: *p<0.05; **p<0.01; ***p<0.001. (B)DTg IAPP$^{+/+}$/APPSwe$^{+/-}$ demonstrate augmented hippocampal Aβ density in comparison to controls STZ injected APP$_{Swe}^{+/-}$ and APP$_{Swe}^{+/-}$. Statistical analysis: One-way ANOVA; p value = 0.0012; Tukey's: **p<0.01.

Colocalization of IAPP and Aβ in Cerebral Plaques in the DTg IAPP$^{+/+}$/APP$_{Swe}^{+/-}$

Very recently, it has been shown that patients affected by T2D and AD display brain Aβ plaques that colocalize with IAPP (57). To analyze the coexistence of both misfolded proteins in the brain of DTg animals, we performed a double immunofluoresce staining to label brain amyloid plaques using antibodies that recognize specifically Aβ and IAPP proteins. In our study, the DTg IAPP$^{+/+}$/APP$_{Swe}^{+/-}$ demonstrated a colocalization between IAPP and Aβ plaques emulating what was recently discovered in human patients. This suggests that IAPP may directly interact with Aβ, acting as a seed, and increasing AD pathology. In Figure 14, immunoreactive IAPP to the anti-IAPP antibody is localized in fluorescent red, and the immunoreactive Aβ to the 82E1 anti-Aβ antibody is seen as fluorescent green. Further confirmation is necessary to validate this co-localization by confocal microscopy. Additionally, looking at Figure 15, there is also a fairly strong linear correlation with the DTg

$IAPP^{+/+}/APP_{Swe}^{+/-}$ and the Het $IAPP^{+/-}/APP_{Swe}^{+/-}$ that the more pancreatic IAPP deposition determines more cortical Aβ burden and vice versa (Figure 15, Pearson Correlation, r = 0.779). Thus, it can be posited that the more IAPP deposition in the mice, the more aggravation in AD pathology. This indicates that IAPP aggregates may directly interact by cross-seeding with Aβ and thereby exacerbate AD pathology.

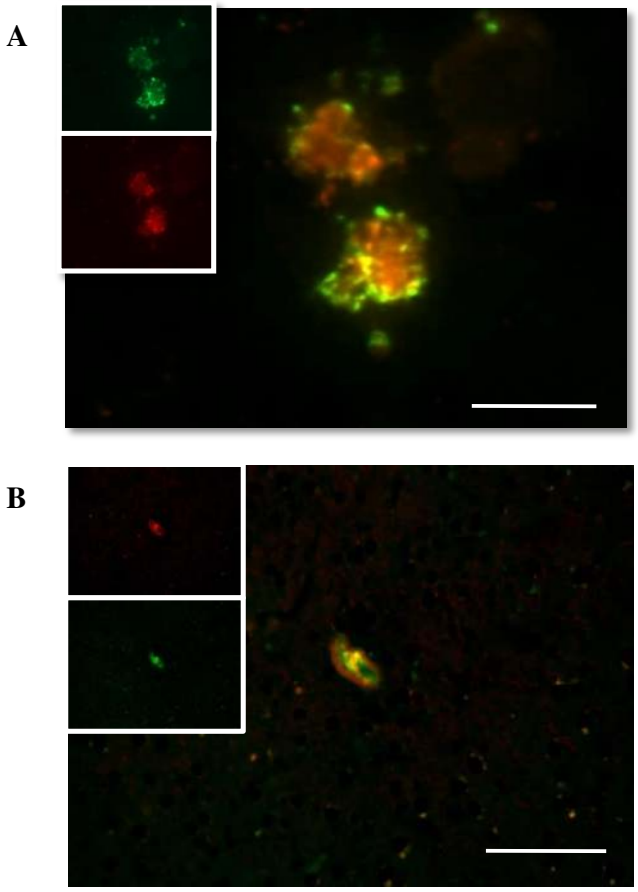

Figure 14. Colocalization of IAPP and Aβ in Cerebral Plaques in the DTg IAPP$^{+/+}$/APP$_{Swe}^{+/-}$. The two following representative images show a colocalization of IAPP (red) and Aβ (green) in the brain parenchyma of the DTg IAPP$^{+/+}$/APP$_{Swe}^{+/-}$ through double immunohistochemistry. IAPP seems to be surrounded by (A) or adjacent to (B) Aβ; nevertheless, IAPP aggregates may interact (yellow) by cross-seeding with Aβ and thereby exacerbate AD pathology. Scale bar: 50 um (A), 100 um (B).

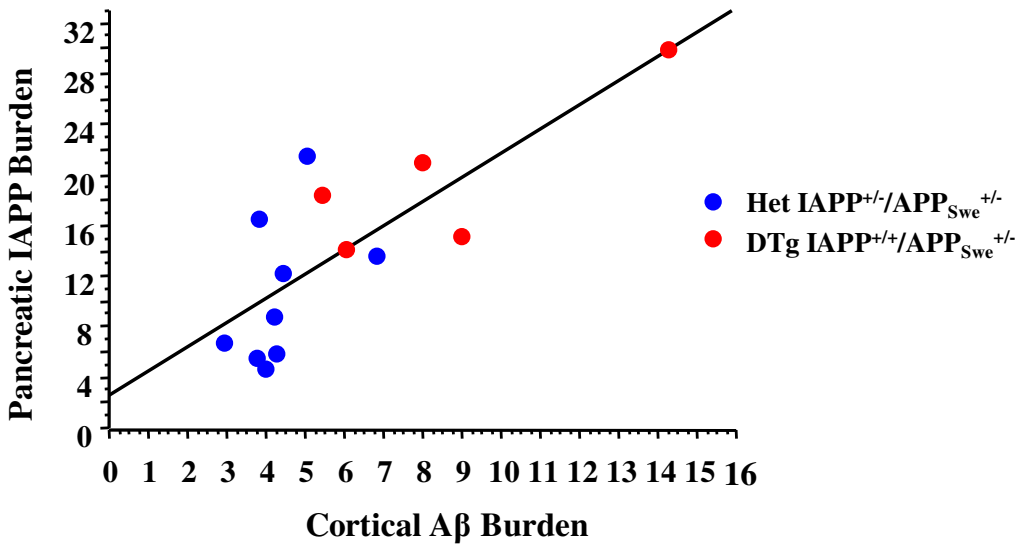

Figure 15. Pancreatic IAPP Burden Correlates with Cortical Aβ Burden in the DTg huIAPP$^{+/+}$/APP$_{Swe}^{+/-}$ and Het IAPP$^{+/-}$/APP$_{Swe}^{+/-}$. This bivariate scatterplot with regression suggests a fairly strong positive linear relationship between pancreatic IAPP burden and cerebral Aβ burden. Thus, if one is heightened, the other is as well. Animals with augmented levels of pancreatic IAPP will cause an increase in cerebral Aβ burden and vice versa. Pancreatic IAPP Burden = 2.602 + 1.916 * Cortical Aβ Burden; R^2= 0.606; Pearson Correlation, r = 0.779

Summary

In this section, we analyzed the effect of IAPP seeds on AD pathology through immunohistochemistry and quantification of cerebral Aβ plaques in the cortex and hippocampus of the DTg $IAPP^{+/+}/APP_{Swe}^{+/-}$, Het $IAPP^{+/-}/APP_{Swe}^{+/-}$, $APP_{Swe}^{+/-}$ injected with STZ (T1D) and $APP_{Swe}^{+/-}$ mice. We found that the DTg $IAPP^{+/+}/APP_{Swe}^{+/-}$ exhibit a proliferation of Aβ burden levels as well as number of Aβ plaques per area in cortical and hippocampal tissue compared to Het $IAPP^{+/-}/APP_{Swe}^{+/-}$, $APP_{Swe}^{+/-}$ injected with STZ (T1D), and $APP_{Swe}^{+/-}$ mice. In addition, the heterozygous $IAPP^{+/-}/APP_{Swe}^{+/-}$ animals had significant cortical Aβ burden levels and Aβ density in comparison to the $APP_{Swe}^{+/-}$ suggesting a dose-dependence of the IAPP expression. Markedly, we were also able to show a colocalization of IAPP and Aβ in cerebral plaques in the DTg $IAPP^{+/+}/APP_{Swe}^{+/-}$ animals corroborating with what was found in T2D-AD patients and non-diabetic AD patients. Analzying the DTg $IAPP^{+/+}/APP_{Swe}^{+/-}$and Het $IAPP^{+/-}/APP_{Swe}^{+/-}$, we are able to see a fairly strong linear correlation between pancreatic IAPP deposition and cortical Aβ corresponding to the more pancreatic IAPP, the more Aβ plaques, confirming that IAPP acting as a seed can intensify AD pathology *in vivo*.

CHAPTER 5

Discussion

Cross-seeding Evidences in T2D and AD.

With pancreatic IAPP aggregation being present in up to 96% autopsied T2D patients (4, 7, 11) and Aβ plaques constantly present in the brain of AD individuals, the importance of exploring these two amyloids cannot be stressed enough. IAPP and Aβ are concomitant as amyloids in PMDs yet implemented in two different diseases affecting disparate areas of the body. IAPP and Aβ both have the propensity to aggregate, have 38% sequence homology (6, 30), and induce cell death (31). Prominently, IAPP and Aβ follow the seeding-nucleation hypothesis, yet with the many similarities they have, we hypothesize that they are able to interrelate with each other and act as a seed to propagate protein misfolding. Our study has shown that cross-seeding of IAPP and Aβ can occur through *in vitro* and *in vivo* methods. Within the test tube, we were able to show that one oligomeric species is able to diminish the nucleation phase, thus speeding up misfolding of the opposite monomeric species. This suggests that these amyloidogenic proteins are able to work both ways to assist each other in the start of misfolding. Our DTg $IAPP^{+/+}/APP_{Swe}^{+/-}$ exhibited an exacerbation in pathology for both diseases – escalation of BGLs, significantly higher pancreatic IAPP, and elevated Aβ burden and density in the cortex and hippocampus.

A plethora of supporting epidemiological and post-mortem studies exists relating T2D and AD in humans, yet it is not well known how one of these diseases could exacerbate the other malady. An epidemiological report studied almost 2,000 individuals without mild cognitive impairment (MCI) and dementia at baseline; however, after a follow-up, a total of 334 individuals had some type of MCI with diabetes being a key player suggesting diabetes is related to a higher risk of amnestic

MCI in a population with an elevated prevalence of this disorder (seen in minorities) (60). Another studies of 65 year and older individuals noted that individuals with T2D were at a higher risk to develop AD (3-4, 22, 61). Our research intended to explain this close association between T2D and AD by a cross-seeding hypothesis, and we demonstrated that animals harboring both amyloidogenic proteins, Aβ and IAPP, showed an early onset and exacerbated development of both diseases, as demonstrated by increased hyperglycemia and higher misfolding protein loads. *In vitro* studies showed that there is acceleration in the aggregation ratio of one protein when the other misfolded protein is present in the system. These results could explain the high incidence of both diseases in the same individuals due to the interaction of Aβ and IAPP.

Histopathological analyses also posit a role of cross-seeding between T2D and AD. It is reported that Aβ and tau are present in the pancreas tissue and in β-cells and Aβ being colocalized with IAPP in islet amyloid aggregates of T2D patients (7, 12 30, 58). Moreover, T2D patients display increased amounts of NFTs and Aβ in the hippocampus (7, 14). In AD patients, there is an extensive prevalence of pancreatic amyloid compared to non-AD (14, 33, 58). In addition, human T2D/AD brains demonstrate an augmented number of cortical Aβ plaques and tau-positive cells compared to affected AD brains suggesting that unified T2D/AD patients have an AD pathology that is more severe with much more of a rapid progression (23). We have observed an increased amount of IAPP load in the pancreas and Aβ load in the brain of double transgenic animals. Indeed, the increase of both burdens is correlated. Furthermore, in Figure 14A, it appears that IAPP is located in the core of this plaque

with an Aβ "halo" surrounding the core. We know that our DTg animals do develop IAPP deposition first, so perhaps, IAPP could be generated in the pancreas, circulate through the blood crossing the BBB, and going to the brain to become our "first seed." These results go along with the observations made in human tissue, indicating that the presence of one of the amyloidogenic proteins raises the aggregation and deposition of the other one, indication a possible cross-seeding effect. Recently, IAPP deposition in the brain was analyzed in T2D/AD patients and AD subjects. IAPP deposition was encountered in the blood vessels and brain parenchyma, and there was a co-localization between IAPP and Aβ in the cortex. This co-localization was higher in affected T2D-AD than AD patients (57). Moreover, we were able to identify a co-localization of Aβ and IAPP in cerebral plaques in the double transgenic animal, very similar to what was described in humans.

Relevance of Study for Novel Therapeutics

Numerous diseases are produced by the accumulation of misfolded aggregated proteins including AD, prion diseases, Parkinson's disease (PD), T2D, and more (16). AD and T2D are so prevalent in our society and with the quantity of elderly and insalubrious lifestyle of individuals increasing in our future, so too does the severity of these diseases. In this study, we are able to emulate in a mouse model the coexistence of both T2D and AD that is reported in affected humans. Moreover, cross-seeding may perhaps explain in part why there is a co-existence of two PMDs in a single patient in a higher prevalence than just by chance as well as the enhanced clinical features in some individuals (15, 33). Cross-seeding processes may explicate why certain disease-affiliated protein aggregates are located in aberrant areas of the affected body (i.e. Aβ

colocalizing with IAPP in the pancreas and IAPP-Aβ co-localization in the brain) (33). These studies allow analyzing the relationship of these diseases and, therefore, aid in developing novel therapeutic strategies by discovering individual disease mechanisms by unlocking knowledge from the relationship between T2D and AD. The advantage of IAPP and Aβ both being amyloids and, therefore, having common structural features, will allow developing new therapeutic interventions to target both proteins, providing more effective drugs. Further information from the synergism of these diseases can possibly alleviate the number of both T2D and AD affected individuals, decrease the prevalence of both of these diseases, and ameliorate the economic burden these diseases place on the world.

CHAPTER 6

Conclusions and Future Directions

Conclusions

In this project, we intended to explore the striking possibility of molecular interaction between two amyloidogenic proteins –IAPP and Aβ- through cross-seeding of protein misfolding by *in vitro* and *in vivo* means. We believe that an enhancement in disease pathology could be due to a cross-seeding effect between IAPP and Aβ and could elucidate the co-existence of T2D and AD cases seen in human patients (3-4, 15, 33, 58-59). We planned to examine how each respective aggregate (Aβ or IAPP) affects the disparate disease pathology through *in vitro* aggregation assays, as well as *in vivo* by immunohistochemcial technique utilizing a novel, double transgenic mouse model that generates both Aβ and IAPP aggregates. Though further investigations are necessary, we can conclude through our preliminary results that:

- We were able to exhibit that protein misfolding and aggregation can be advanced through homologous and heterologous seeding by utilizing synthetic peptides for both diseases where IAPP oligomeric species incubated with synthetic Aβ-42 and Aβ-42 oligomers incubated with synthetic IAPP were able to accelerate protein misfolding and aggregation. Each of these heterologous seeds, were able to shorten the lag phase for polymerization indicating the existence of a cross-seeding mechanism between Aβ and IAPP in both directions *in vitro*.
- To determine the influence of Aβ aggregate "seeds" on T2D pathology in a double transgenic mouse model, the DTg $IAPP^{+/+}/APP_{Swe}{}^{+/-}$ mice have significantly elevated BGLs in comparison to the control Het $IAPP^{+/-}/APP_{Swe}{}^{+/+}$,

$IAPP^{+/+}$, and $IAPP^{+/-}$. This indicates that the presence of Aβ peptide is able to aggravate T2D symptoms (hyperglycemia) in an *in vivo* model.

- IAPP burden levels in the pancreas are highest in DTg $IAPP^{+/+}/APP_{Swe}^{+/-}$ animals in comparison to the Het $IAPP^{+/-}/APP_{Swe}^{+/+}$ and $IAPP^{+/+}$ by immunohistochemical and quantification analysis. The heterozygous $IAPP^{+/-}/APP_{Swe}^{+/-}$ mice have T2D-like pathology, although heterozygous $IAPP^{+/-}$ do not develop any diabetic-like pathology at any age. Thus, the mere presence of Aβ peptide in the diabetic animals induces a higher deposition of IAPP in the pancreas confirming a possible close relationship between Aβ and IAPP aggregation.
- To evaluate the influence of IAPP aggregate "seeds" on AD pathology in a double transgenic mouse model, the DTg $IAPP^{+/+}/APP_{Swe}^{+/-}$ exhibit increased cortical and hippocampal Aβ burden levels; and Aβ plaque density compared to controls through Aβ immunostaining. These results indicate that the presence of misfolded IAPP in the brain exacerbates AD pathology in DTg animals. In addition, colocalization between IAPP and Aβ was seen in DTg $IAPP^{+/+}/APP_{Swe}^{+/-}$ cerebral plaques. Moreover, there is also a fairly strong linear correlation with the DTg $IAPP^{+/+}/APP_{Swe}^{+/-}$ and the Het $IAPP^{+/-}/APP_{Swe}^{+/-}$ that the more pancreatic IAPP deposition determines more cortical Aβ burden and vice versa. This indicates that IAPP aggregates may directly interact by cross-seed with Aβ and thereby exacerbate AD pathology.

Future directions

Characterization and Quantification of *In Vitro* Cross-seeding.

Currently, after obtaining putative homologous and heterologous seeding *in vitro* assay, we plan to characterize and quantify the cross-seeding assay through use of immunogold labeling and TEM which will allow us to contrast the two proteins, as well as dot blot after fractionation and/or sedimentation assay to quantify the soluble and insoluble peptide for both IAPP and Aβ seeding assays. Utilizing immunogold labeling will result in colloidal gold particles binding to these proteins, and due to gold's high electron density, it escalates electron scatter resulting in high contrast allowing us to use TEM to conjugate by IAPP and Aβ's different size. For the immunogold labeling plus TEM, we want to prove that IAPP and Aβ are localized in the same polymer. There is difficulty in quantifying these assays; thus, we can attempt a sedimentation assay. Briefly, in the sedimentation assay, two reactive antibodies to recognize IAPP and Aβ will be incubated with the fractionated proteins with different time points taken in order to quantify the protein concentration of both proteins. In addition, further work is necessary such as addition of more controls - incubation with the opposing monomeric seed-free or incubation with a different proteins aggregate (i.e. albumin).

Biochemical Quantification of Amyloids in Brain and Pancreas.

Additionally, we will perform biochemical analysis of the brain and pancreas homogenates to quantify the IAPP and Aβ levels in each tissue. We will utilize enzyme-linked immunosorbent assay (ELISA) measurements of Aβ-42 (in brain) and IAPP (pancreas) from the animal groups. For our case, we will use a two-step fractionation in

which we will centrifuge brain or pancreatic homogenate to obtain a PBS solvent soluble fraction that will measure soluble monomers/oligomers, and a formic acid solvent insoluble fraction measuring insoluble aggregates which refer to aggregated forms. Then, we will run brain and pancreas through both ELISAs 1) recognizing human Aβ and 2) recognizing human IAPP. Briefly, to make each tissue homogenate, mouse brain/pancreas will be weighed and calculated to add 10% of the weight/volume of PBS containing protease inhibitor. The brain/pancreas will be homogenized and frozen in liquid nitrogen and stored at -80 °C until use. Homogenate will be placed in Beckman centrifuge tubes and centrifuged at 32,600 rpm at 4°C for 1 hour. The PBS supernatant will be collected and frozen in liquid nitrogen. The insoluble pellet will be transferred and resuspended in formic acid solution. The sample is then sonicated to obtain an apt homogenous solution. After sonication, the samples are once again centrifuged. The formic acid fraction is collected, diluted in EC buffer, frozen in liquid nitrogen, and stored at -80 °C until use for ELISA quantification.

Exogenous Cross-seeding of Aβ on T2D and IAPP on AD.

To further investigate our cross-seeding hypothesis between in Aβ in AD and IAPP in T2D, we plan to exogenously induce cross-seeding *in vivo* by adding external seeds (peripherally and intracerebrally). The idea is to introduce exogenously heterologous IAPP seeds in Tg animals of AD ($APP_{Swe}^{+/-}$ or Tg2576) and Aβ seeds in T2D ($huIAPP^{+/+}$) and exacerbate the disease's pathology. It has been reported that *in vivo* amyloidogenic heterologous oligomers can be injected and are able to accelerate the seeding process. In our laboratory, Tg2576 animals and WT littermates were injected intra-peritoneally (i.p.) with RML prions at 45 and 365 days old. The Tg2576

mice developed clear clinical signs of prion disease quicker than the non-Tg controls; in addition, misfolded prion protein (PrP^{Sc}) formation was accelerated in prion-injected Tg2576, as well (33). Aβ is proven to generate AD under experimental conditions, yet IAPP is unknown. Another example, amyloid beta-derived diffusible ligands (ADDLs) were injected into the brain and diffused throughout the brain - even in newly formed aggregated plaques (19, 26). Our lab has recapitulated this by injecting different tissues (brain, blood, pancreas), models (Tg2576, APP/PS1, huIAPP), and different proteins (synthetic Aβ, IAPP). In this future experiment to demonstrate the cross-seeding effect of Aβ on IAPP aggregates, we will take the previously described $huIAPP^{+/+}$ mice and inject by i.p. route human AD patient or aged Tg2576 brain homogenates, as well as healthy human and aged non-transgenic littermates brain homogenates in $huIAPP^{+/+}$ mice for controls. Other control groups will likely be implemented including another PMD inoculum such as PD in order to see if one is a stronger seed than the other, as well as a non-PMD brain disease, such as hydrocephalus or schizophrenia. The animals will be injected at 3 weeks of age, and the progression of a diabetes-like pathology will be followed overtime by taking BGL overtime; insulin resistance will be measured at the age of 16 weeks. The animals will be sacrificed at 20 weeks of age (Figure 16). This is the age when T2D pathological actions start to appear in the $huIAPP^{+/+}$ mice; thus, we will be able to analyze the additive effect of exogenously introduced Aβ deposits in the development in T2D. The pancreatic tissue will be assayed by utilizing immunohistochemical and biochemical techniques. We expect to see a more robust acceleration of IAPP deposition in the pancreas and more severe T2D clinical signs in

the AD homogenate i.p. injected animals compared to the healthy homogenate injected animals with both human and mouse inocula.

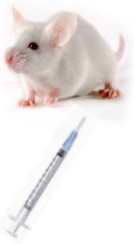

n = 7 each, huIAPP$^{+/+}$ injected with AD human brain or with normal human brain
n = 7 each, huIAPP$^{+/+}$ injected with aged Tg2576 brain or aged non-transgenic brain
n = 7 each, huIAPP$^{+/+}$ injected with alternate PMD or non-PMD

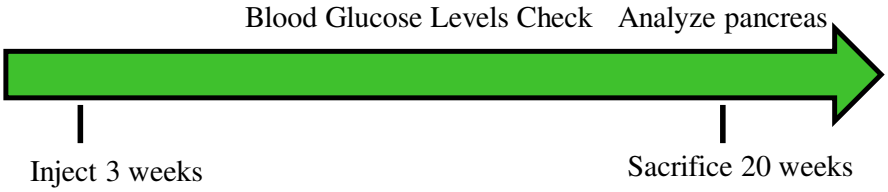

Figure 16. Exogenous Cross-seeding of Aβ on T2D. This figure shows the timeframe of this experiment to introduce Aβ seeds through i.p. injection 100 µL of AD human or aged Tg2576 in huIAPP$^{+/+}$ mice (n=7/group). Animals will be injected at 3 weeks of age, insulin resistance will be assessed at 16 weeks and will be sacrificed at 20 weeks checking BGLs monthly overtime.

To demonstrate the cross-seeding effect of IAPP on AD pathology, we will introduce IAPP seeds exogenously by injecting human T2D pancreas or aged huIAPP$^{+/+}$ pancreas homogenate through intra-cerebral (i.c.) route into the previously described Tg2576 AD model. Tg2576 (n=7/group) will be injected at 2 months of age with either human: T2D pancreas, T1D pancreas, and healthy pancreas; or mouse: aged huIAPP$^{+/+}$ pancreas, or aged–matched WT pancreas treated with STZ (T1D), and non-diabetic WT

pancreas will be injected. A group of WT animals will be injected i.p. with Streptozotocin (STZ) to create a T1D mouse model, and the pancreas homogenate of these animals will be injected i.c. in order to create a Type 1 diabetic control injected group. This is a relevant control in that it will help elucidate the role of amylin and create a homogenate to be injected with a paucity of amylin without aggregates. Behavior will be assessed at 8.5 months by the hippocampal dependent Barnes maze, before any AD pathology would normally occur in these animals, and sacrificed at 9 months (Figure 17). TopScan 2.0 tracking software will be used to track the animal's movements, as well as data will be analyzed utilizing GraphPad Prism. The brain will be assayed by utilizing immunohistochemical and biochemical techniques to analyze any anomalies in the disease-like pathology of these Tg2576 animals. We expect to see a more robust acceleration in the T2D homogenate i.c. injected animals compared to the healthy homogenate and T1D induced.

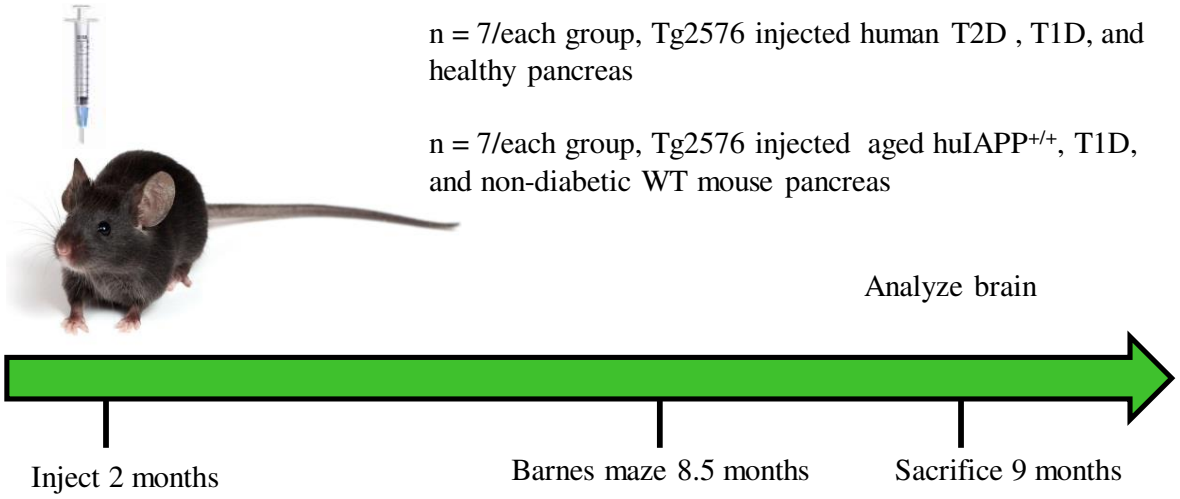

Figure 17. Exogenous Cross-seeding of IAPP on AD and Aβ Aggregates. This figure shows the timeframe of this experiment to introduce IAPP seeds through i.c. injection 10 µL of aged huIAPP$^{+/+}$ pancreas in Tg2576 mice (n=7/group). Animals will be injected at 2 months of age and will be sacrificed at 9 months. Behavior will be assessed at 8.5 months by Barnes maze.

CHAPTER 7

Materials and Methods

***In Vitro* Aβ-42 and IAPP Preparation and Aggregation.**

Aβ (1-42) synthetic peptide powder (Yale University) was dissolved (1 mg/mL) in 50/50 acetonitrile and water, frozen in liquid nitrogen, and lyophilized overnight. Next, the lyophilized Aβ was then dissolved 400 µl/mg in 10 mM NaOH (~pH 12) and vortexed. The high pH is away from Aβ's isoelectric point (~pH 5.5) which will prevent Aβ from aggregating (62). Using a 30 KDa cut-off filter, the material was centrifuged for 12 min. at 14,000 X g at 4°C. This guarantees the solution will contain just be monomeric Aβ form, but not oligomers, so called "seed-free". To quantify the protein concentration, BCA assay (Micro BCA Protein Assay, ThermoScientific) was used. Small aliquots were made and stored at -80 °C until use. Next, we ran an aggregation assay to test the quality of our Aβ seeds. Our Aβ seeds were diluted at different concentrations (1 µM, 2 µM, and 5 µM) in 10 mM NaOH (~pH 12) to determine the impeccable concentration to use for establishing a practical standard curve with an appropriate lag phase; thus, when we added the IAPP aggregates for the cross-seeding assay, we would see an acceleration in the lag phase demonstrating quicker amyloid accumulation compared to the standard curve. 100 µl of Tris-Cl (200 mM, pH 7.4) buffer was added to each well of a 96-well standard opaque plate on ice as well as 20 µg of monomeric Aβ-42 seed-free in each well. 10% and 1% of IAPP oligomers of the 20 µg of Aβ-42 seed-free was added; the control was an insertion of the buffer the oligomer was originated with the final volume brought to 180 µl by adding sterile filtered water. 20 µl of 50 µM Thioflavin T (ThT) was added, and the fluorescence read by a fluorometer at excitation 435 and emission 485 nm with intensity over time. The ThT assay is a well-established *in vitro* staining for amyloid that recognizes and binds

amyloid fibrils; thus, when bound, the ThT emission peak changes allowing us to monitor amyloid formation (55). The plate was covered and shaken with cyclic agitation (500 rpm x 1 minute / no shaking 29 minutes) at 20°C while reading fluorescence every 24 hours or so.

IAPP synthetic peptide powder (Yale University) was dissolved (1 mg/mL) in 50/50 acetonitrile and water, frozen in liquid nitrogen, and lyophilized overnight. Next, the lyophilized IAPP was then dissolved 400 µl/mg in 2 mM HCl (~pH 2) and vortexed. As previously described, a 30 KDa cut-off filter was used to filter and then the material was centrifuged for 12 min. at 14,000 X g at 4°C. To quantify the protein concentration, BCA assay was used. Small aliquots were made and stored at -80 °C until use. Next, we ran an aggregation assay to test the quality of our IAPP seeds following the same reason as above – to establish a template standard curve. One deterrent is the fact that IAPP is known to aggregate much quicker than Aβ; thus, it would be challenging to obtain a standard curve with a suitable lag phase. This was accomplished by the ThT Assay was done by adding 8 µg of prepared IAPP seed-free and buffer per well in a 96-well standard opaque plate on ice in sextuplicates. 10% and 1% of Aβ oligomers from the 8 µg of IAPP seed-free was added for the heterologous oligomeric seeds with the control being supplemented with the buffer the oligomer was originated (100 mM Tris-Cl). 20 µl of 50 µM ThT was added, and the plate was covered and shaken with cyclic agitation (450 rpm x 1 minute / no shaking 29 minutes) at 20°C while reading fluorescence over time by a fluorometer at excitation 435 and emission 485 nm every hour or so.

***In vitro* Aβ and IAPP Oligomer Preparation.**

The aliquoted Aβ and IAPP seed-free peptide was diluted to a final concentration of 0.05 μg/μL in 100 mM Tris-Cl, pH 7.4. 400-500 μL of the diluted solution was placed in an Eppendorf low-binding tube and thermomixed at 25°C, 450 rpm for 5 hours. After the 5 hours, small aliquots (20-30 μL) were made and stored at -80°C until further use for the seeding experiments. For IAPP oligomer preparation, the aliquoted IAPP seed-free peptide was diluted to a final concentration of 0.04 μg/μL in 100 mM Tris-Cl buffer. 400-500 μL of the diluted solution was placed in an Eppendorf low-binding tube and mixed at room temperature for 450 rpm for 90 minutes. After the 90 minutes, small aliquots (20-30 μL) were made and stored at -80°C until further use for the seeding experiments. For both peptides, the concentration of oligomers was measured by BCA.

Animal Models.

The AD transgenic mouse model Tg2576 (Jackson Laboratories) are heterozygous animals on a S129 background over-expressing the 695 amino acid isoform of human APP harboring a double mutation ($Lys^{670} \rightarrow Asn$, $Met^{671} \rightarrow Leu$) found in a large Swedish family with early-onset AD. These animals have a 5-fold Aβ-40 and 14-fold Aβ-42 production and have behavioral impairments and amyloid accumulation around 9-10 months (56). The generation and initial characterization of these mice has been reported previously (56). The human IAPP (huIAPP) homozygous transgenic mouse (Ins2-IAPP1) is a T2D animal model that over-expresses human IAPP on a FVB background. These animals are characterized as developing diabetic-like traits such as high BGLs, impaired insulin secretion, β-cell death, and aggregation of

IAPP at around 20 weeks of age. Important to note, the heterozygous have not been reported to develop islet amyloid deposits or spontaneous T2D (25). The generation and initial characterization of these mice has been previously reported (25). To study the possibility of cross-seeding of protein misfolding on the synergistic interaction between T2D and AD, we generated T2D/AD DTg mice by breeding these transgenic models of both maladies. We crossed the T2D-like huIAPP/FVB mouse with the Tg2576/S129 AD model in which the founders gave us a set of viable heterozygotes that were then backcrossed with the parental homozygous transgenic huIAPP to yield a F2 generation of varied genetic constructs, including the DTg $IAPP^{+/+}/APP_{Swe}^{+/-}$ model that harbors 2 copies of human IAPP and one copy of human mutant APP. From the F2 generation, we also obtained the Het $huIAPP^{+/-}/APP_{Swe}^{+/-}$, $huIAPP^{+/-}$, and the $huIAPP^{+/-}$ mice. The exact huIAPP genetic load of the DTg animals and non-transgenic littermates for controls was reassured by quantitative PCR (Jackson Laboratories). All groups are composed by 5-7 animals. Since amyloid plaques start to appear around 9 months old, the transgenic animals were sacrificed at 8 months and 20 days to be able to analyze the acceleration of brain amyloidosis before their regular pattern of deposition. Before sacrificing the animals, BGLs were measured by a tail vein nick using Contour blood glucose test strips (Bayer Healthcare) after 16 hours of fasting. The animals were then sacrificed by CO_2 inhalation and intracardially perfused with 5 μM anticoagulant Ethylenediaminetertraacetic acid (EDTA) PBS buffer at 250 days old extracting the brain and pancreas to analyze through immunohistochemistry. One half of each tissue was post-fixed in formalin while the other half was snap-frozen and kept at -80 °C. Animals were housed in groups of up to 5 in individually ventilated cages under

standard conditions (22 °C, 12 hour light–dark cycle) receiving food and water ad libitum. All animal experiments were approved by the Institutional Animal Care and Use Committee at The University of Texas Health Science Center in Houston Medical School and accordance with NIH regulations.

Generation of STZ Injected $APP_{Swe}^{+/-}$ (T1D Control).

For a T1D control we had a set of animals that develop clinical signs of diabetes (hyperglycemia and low insulin production by β-cell death) but without over-expression of human IAPP. This would prove that the augmented AD pathology is due to aggregated IAPP and not to the hyperglycemic environment or the reduction of insulin levels that also happen in the huIAPP animal model. STZ is known to be toxic to insulin-producing β-cells when injected and ultimately destroys them, resulting in a diabetic model with increased hyperglycemia. STZ (Sigma-Aldrich) was diluted in sodium citrate buffer (10mM, pH 4.5) and injected intraperitoneally at 110 mg/kg per day during two consecutive days to the overnight fasted $APP_{Swe}^{+/-}$. Animals were sacrificed at 8 months and 20 days of age.

Immunohistochemistry (IHC).

Brain and pancreas were removed, post-fixed into fixative solution (10% formalin) and embedded in paraffin. Briefly, after one week post-fixation in formalin, tissues were dehydrated in serial graded alcohol, immersed in xylene and embedded in paraffin. Serial 10 μm-thick sections from all animal groups (5 sections/stain/animal) were processed in parallel for immunostaining using the same solutions to minimize variability in staining conditions. Tissue was paraffin embedded and sliced by microtome mid-sagitally at 10μm. Sample slides were then deparaffinized and hydrated.

Briefly, slides were immersed in xylene for 15 min, in 100% ethanol, 95% ethanol, 90% ethanol, 80% ethanol, 70% ethanol, and dH_2O for about 5 min each followed by three PBS for 5 min. After blocking the endogenous peroxidase activity with 3% H_2O_2 - 10% methanol in PBS, pH 7.4, for 20 min and washed, slides were incubated overnight in primary antibody mouse IgG anti-human Aβ 82E1 1:1000 (IBL) and/or rabbit anti-amylin [25-37] 1:1000 (Peninsula Laboratories) in PBS Triton Buffer 0.2%. After washing, primary antibody was detected by incubating 1 hour at room temperature in PBS Triton Buffer 0.2% and Alexa Fluor 488 goat anti-mouse (to visualize Aβ) and/or 594 goat anti-rabbit (to visualize IAPP). Finally, after washing, slides were covered with mounting medium with DAPI (Vector) and visualized under an epifluorescent microscope (DMI6000B, Leica) and analyzed in Image J software.

Image Analysis.

Images were taken using a Leica DMI600 microscope at 20X objective for pancreas and 5X for hippocampus and cortex with threshold intensity remaining constant. We analyzed the hippocampus and cortex due to the extensive reports of AD pathology affecting chiefly these regions in transgenic mice and human patients (16, 27). Photomicrographs were taken and imported to Image J 1.45s software and converted into black and white images. Pancreas and brain areas are outlined and the number of pixels is enumerated, and those units converted into um^2 for quantification. For pancreatic IAPP burden calculations, we use the percentage of area stained to total area for IAPP load. In the brain, we quantify Aβ burden and Aβ plaque number and density. Aβ burden/load is quantified by the percentage of area stained to total area analyzed. Aβ plaque density is measured as how many plaques per area analyzed

utilizing scaled measurements. Each analysis was done by a single examiner blinded to sample identities.

Statistical Analysis.

Graphs are expressed as means ± standard error of the mean (s.e.m.). After confirming normal distribution with Skewness and Kurtosis statistic test, one way analysis of variance (ANOVA) followed by a post-hoc Tukey's multiple comparisons test were used to analyze differences among groups. For linear correlation, Pearson correlation coefficient was used. Statistical differences for all tests were considered significant at the $p<0.05$ level. Statistical analysis was performed using GraphPad Prism 5.0 software (GraphPad Software Inc).

Chapter 8

Appendix

Bibliography

1. American Diabetes Association, 2011. National Diabetes Fact Sheet 2011. Diabetes Public Health Resource. Available at http://www.cdc.gov/diabetes/pubs/pdf/ndfs_2011.pdf, July 2012.
2. Alzheimer's Association. 2012 Alzheimer's disease Facts and Figures. Alzheimer's and Dementia 8 (2): 14-16 (2012).
3. Ott A., Stolk R.P., Hofman A., van Harskamp F., Grobbee D.E., Breteler M.M. Association of Diabetes mellitus and dementia: the Rotterdam Study. Diabetologia 39: 1392-7 (1996).
4. Ott A., Soltk R.P., van Harskamp F., Pots H.A., Hofman A., Breteler M.M. Diabetes mellitus and the risk of dementia: the Rotterdam Study. Neurology 53: 1937-42 (1999).
5. Reila R., Rodriguez B.L., Launer L.J. Type 2 Diabetes, APOE gene, and the risk for dementia and related pathologies: the Honolulu-Asia Aging Study. Diabetes 51: 1256-62 (2002).
6. Nicolls M. The Clinical and Biological Relationship between Type II Diabetes mellitus and Alzheimer's disease. Current Alzheimer's Research 1: 447-54 (2004).
7. Miklossy J., Qing H., Radenovic A., Kis A., Vileno B., Laszlo F., Miller L., Martins R.N., Waeber G., Mooser V., Bosman F., Khalili K., Darbinian N., McGeer P. L. Beta amyloid and hyperphosphorylated tau deposits in the pancreas in type 2 diabetes. Neurobiol Aging 31: 1503-1515 (2010).

8. Sims-Robinson C., Kim B., Rosko A., Feldman E.L. How does diabetes accelerate Alzheimer's disease pathology? Nat Rev Neuro 6: 551-59 (2010).
9. DeFronzo R. Pharmacologic therapy for type 2 diabetes mellitus. Ann Intern Med. 133:73–74 (2000).
10. Luchsinger J., Gustafson D. Adiposity, type2 diabetes and Alzheimer's disease. J Alzheimer's Dis. 16(4):693-704 (2009).
11. Clark A., de Koning E.J., Hattersley A.T., Hansen B.C., Yajnik C.S., Poulton J. Pancreatic pathology in non-insulin dependent diabetes (NIDDM). Diabetes Res Clin Pract 28: S39-47 (1995).
12. Montane J., Klimek-Abercrombie A., Potter K.J., Westwell-Roper C., Verchere C.B. Metabolic Stress, IAPP, and Islet Amyloid. Diabetes, Obesity and Metabolism 14: 68-77 (2012).
13. Westermark P. Amyloid in the islets of Langerhans: thoughts and some historical aspects. Ups J Med Sci Suppl 116: 81-89 (2011).
14. Akter K., Lanza E.A., Martin S.A., Myronyuk N., Rua M., Raffa R.B. Diabetes mellitus and Alzheimer's disease: shared pathology and treatment? Bri J Clin Pharmacol 71(3): 365-76 (2011).
15. Valente T., Gella A., Fernández-Busquets X., Unzeta M., Durany N. Immunohistochemical analysis of human brain suggests pathological synergism of Alzheimer's disease and diabetes mellitus. Neurobiol Dis 37: 67-68 (2010).
16. Soto C. Unfolding the role of protein misfolding in neurodegenerative diseases. Nat Rev Neuro 4: 49-60 (2003).

17. Moreno-Gonzalez I., Soto C. Misfolded protein aggregates: mechanisms, structures, and potential for disease transmission. Sem Cell Dev Biol 22:482-487 (2011).
18. Chiu S.L., Chen C.M., Cline H.T. Insulin receptor signaling regulates synapse number, dendritic plasticity, and circuit function in vivo. Neuron 58: 708-19 (2004).
19. Kroner Z. The Relationship between Alzheimer's Disease and Diabetes: Type 3 Diabetes? Alt. Med. Review 14(4):373-77 (2009).
20. O'Brien T.D., Butler P.C., Westermark P., Johnson K.H. Islet amyloid polypeptide: a review of its biology and potential roles in the pathogenesis of diabetes mellitus. Vet Pathol 30 (4): 317-332 (1993).
21. Hayden M., Tyagi S.C. "A" is for Amylin and Amyloid in Type 2 Diabetes Mellitus. JOP 2(4): 124-139 (2001).
22. Banks W.A., Kastin A.J., Maness L.M., Huang W., Jaspan J.B. Permeability of the Blood-Brain Barrier to Amylin. Life Sci 57 (22): 1993-2001 (1995).
23. Bretherton-Watt D., Bloom S.R. Islet Amyloid Polypeptide: The Cause of Type-2 Diabetes? TEM 2(6): 203-207 (1991).
24. Narita R., Toshimori H., Nakazato M., Kuribayashi T., Toshimori T., Kawabata K., Takahashi K., Masukura S. Islet amyloid polypeptide (IAPP) and pancreatic islet amyloid deposition in diabetic and non-diabetic patients. Diabetes Res Clin Pract 15: 3-14 (1992).

25. Janson J., Soeller W.C., Roche P.C., Nelson R.T., Torchia A.J., Kreutter D.K., Butler P.C. Spontaneous diabetes mellitus in transgenic mice expressing human islet amyloid polypeptide. Proc Natl Acad Sci USA 93: 7283-7288 (1996).
26. Gaspar R.C., Villarreal S.A., Bowles N., Hepler R.W., Joyce J.G., Shughrue P.J. Oligomers of β-amyloid are sequestered into and seed new plaques in the brains of an AD mouse model. Exp Neurol 223: 394-400 (2010).
27. Meredith S.C. Protein Denaturation and Aggregation: Cellular Responses to Denatured and Aggregated Proteins. Ann N.Y. Acad Sci 1066: 181-221 (2005).
28. Han W., Li C. Linking type 2 diabetes and Alzheimer's disease. Proc Natl Acad Sci USA 107(15):6557-58 (2010).
29. Kimura R., MacTavish D., Yang J., Westaway D., Jhamandas J.H. Beta Amyloid-Induced Depression of Hippocampal Long-Term Potentiation is Mediated through the Amylin Receptor. J Neurosci 32(48): 17401-17406 (2012).
30. Andreetto E., Yan L.M, Tatarek-Nossol M., Velkova A., Frank R., Kapurniotu. Identification of Hot Regions of the Aβ-IAPP Interaction Interface as High-Affinity Binding Sites in both Cross-and Self-Association. Angew Chem Int Ed. 49: 3081-85 (2010).
31. Fu W., Ruangkittisakul A., MacTavish D., Shi J.Y., Ballanyi K., Jhamandas J.H. Amyloid-beta (Aβ) peptide directly activates Amylin-3 receptor subtype by triggering multiple intracellular signaling pathways. J Biol Chem 287 (22): 18820-30 (2012).

32. Soto C., Frangione B. Two conformational states of amyloid beta-peptide: implications for the pathogenesis of Alzheimer's disease. Neurosci Lett 186 (2-3): 115-118 (1995).
33. Morales R., Moreno-Gonzalez I., Soto C. Cross-seeding of Amyloids: Implications in Pathogenesis and Sporadic Disease. (in press).
34. Rochet J., Lansbury Jr. P.T. Amyloid fibrillogenesis: themes and variations. Curr Op in Struct Bio 10: 60-68 (2000).
35. Jucker M., Walker L.C. Pathogenic Protein Seeding in Alzheimer's Disease and Other Neurodegenerative Disorders. Ann Neurol 70(4): 532-40 (2011).
36. Soto C., Estrada L., Catilla J. Amyloids, prions and the inherent infectious nature of misfolded protein aggregates. Trends Biochem Sci 31: 150-55 (2006).
37. Morales R., Estrada L.D., Diaz-Espinoza R., Morales-Scheining D., Jara M.C., Castilla J., Soto C. Molecular Cross talk between misfolded proteins in animal models of Alzheimer's and prion diseases. J Neurosci 30 (13): 4528-35 (2010).
38. Tsigelny I.F., Crews L., Desplats P., Shaked G.M., Sharikov Y., Mizuno H., Spencer B., Rockenstein E., Trejo M., Platoshyn O., Yuan J.X., Masliah E. Mechanisms of hybrid oligomer formation in the pathogenesis of combined Alzheimer's and Parkinson's diseases. PLos ONE 3 (9):e3135 (2008).
39. Clinton L.K., Blurton-Jones M., Myczek K., Trojanowski J.Q., LaFerla F.M. Synergistic interactions between Abeta, tau, and alpha-synuclein: acceleration of neuropathology and cognitive decline. J Neurosci 30: 7281-7289 (2010).

40. Ono K., Takahashi R., Ikeda T., Yamada M. Cross-seeding effects of amyloid β-protein and α-synuclein. J Neurochem 122 (5): 833-90 (2012).
41. Gotz J., Chen F., Van Dorpe J., Nitsch R.M. Formation of neurofibrillary tangles in P301l tau transgenic mice induced by Abeta 42 fibrils. Science 293: 1491-1495 (2001).
42. Lewis J., Dickson D.W., Lin W.L., Chisholm L., Corral A., Jones G., Yen S.H., Sahara N., Skipper L., Vager D., Eckman C., Hardy J., Hutton M., McGowan E. Enhanced neurofibrillary degeneration in transgenic mice expressing mutant tau and APP. Science 293: 1487-1491 (2001).
43. Biancalana M., Koide S. Molecular Mechanism of Thioflavin-T Binding to Amyloid Fibrils. Biochem Biophys Acta 1804(7): 1405-1412 (2010).
44. O'Nuallain B., Williams A.D., Westermark P., Wetzel R. Seeding Specificity in Amyloid Growth Induced by Heterologus Fibrils. J Biol Chem 279 (17): 17490-17499 (2004).
45. Kayed R., Bernhagen J., Greenfield N., Sweimeh K., Brunner H., Voelter W., Kapurniotu A. Conformational Transitions of Islet Amyloid Polypeptide (IAPP) in Amyloid Formation *in vitro*. J Mol Biol 287: 781-796 (1999).
46. Chargé S., de Koning E.J.P., Clark A. Effect of pH and insulin on fibrillogenesis of islet amyloid polypeptide in vitro. Biochem 34: 14588-14593 (1995).
47. Kapurniotu A., Bernhagen J., Greenfield N., Al-Abed Y., Teichberg S., Frank R., Voelter W., Bucala R. Contribution of advanced glycosylation to the

amyloidogenicity of islet amyloid polypeptide (IAPP). Eur J Biochem 251: 208-216 (1998).

48. Padrick S.B., Miranker A.D. Islet Amyloid: Phase Partitioning and Secondary Nucleation Are Central to the Mechanism of Fibrillogenesis. Bich 41: 4694-4703 (2002).
49. Clark M.J., Jr., Sterrett J.J., Carson D.S. Diabetes Guidelines: A Summary and Comparison of the Recommendations of the American Diabetes Association, Veterans Health Administration, and American Association of Clinical Endocrinologists. Clin Ther 22: 899–910 (2000).
50. American Diabetes Association, 2012. Standards of Medical Care in Diabetes – 2012. Diabetes Care 35: Suppl S11-63 (2012).
51. Fox N., Schrementi J., Nishi M., Ohagi S., Chan S.J., Heisserman J.A., Westermark G.T., Leckstrom A., Westermark P., Steiner D.F. Human islet amyloid polypeptide transgenic mice as a model of non-insulin-dependent diabetes mellitus (NIDDM). FEBS Lett 323: 40-44 (1993).
52. de Koning E.J.P., Hoppener J.W.M., Verbeek J.S., Oosterwijk C., van Hulst K.L., Baker C.A., Lips C.J.M., Morris J.F., Clark A. Human islet amyloid polypeptide accumulates at similar sites in islets of transgenic mice and humans. Diabetes 43: 640-644 (1994).
53. Yagui K., Yamaguchi T.,Kanatsuka A., Shimada F., Huang C.I., Tokuyama Y., Ohsawa H., Yamamura K.I., Miyazaki J.I., Mikata A., Yoshida S., Makino H. Formation of islet amyloid fibrils in beta-secretory granules of

transgenic mice expressing human islet amyloid polypeptide/amylin. Eur J Endocrinol. 132: 487-496 (1995).

54. Couce M., Kane L.A., O'Brien T.D., Charlesworth J., Soeller W., McNeish J., Kreuuter D., Roche P., Butler P.C. Treatment with growth hormone and dexamethasone in mice transgenic for human islet amyloid polypeptide causes islet amyloidosis and beta-cell dysfunction. Diabetes 45(8): 1094-101 (1996).
55. Tesch G.H., Allen T.J. Rodent models of streptozotocin-induced diabetic nephropathy. Nephrology 12: 261-266 (2007).
56. Hsiao K., Chapman P., Nilsen S., Eckman C., Harigaya Y., Younkin S., Fusheng Y., Cole G. Correlative Memory Deficits, Aβ Elevation, and Amyloid Plaques in Transgenic Mice. Science 274: 99-102 (1996).
57. Jackson K., Barisone G.A., Diaz E., Jin L., DeCarli C., Despa F. Amylin deposition in the brain: a second amyloid in Alzheimer's disease? Annal of Neuro (in publication) (2013).
58. Janson J., Laedtke T., Parisi J.E., O'Brien P., Peterson R.C., Butler P.C. Increased risk of type 2 diabetes and Alzheimer's disease. Diabetes 53: 474-481 (2004).
59. Jhamandas J.H., Li Z., Westaway D., Yang J., Jassar S., MacTavish D. Actions of β-Amyloid Protein on Human Neurons Are Expressed through the Amylin Receptor. Amer J Pathol 178 (1): 140-49 (2011).
60. Luchsinger, J.A., Reitz C., Patel B., Tang M., Manly J.J., Mayeux R. Relation of Diabetes to Cognitive Impairment. Arch Neurol 64(4): 570-575 (2007).

61. Yoshitake T., Kiyohara Y., Kato I., Ohmura T., Iwamoto H., Nakayama K., Ohmori S., Nomiyama K., Kawano H., Ueda K. Incidence and risk factors of vascular dementia and Alzheimer's disease in a defined elderly Japanese population: the Hisayama Study. Neurology: 45(6): 1161-8 (1995).
62. Bitan G., Lomakin A., Teplow D.B. Amyloid-β Protein Oligomerization: Prenucleation Interactions Revealed by Photo-Induced Cross-Linking of Unmodified Proteins. J Biol Chem 276: 35176-184 (2001).

VITA

George Edwards III, son of George Edwards, Jr. and Donna Joswiak, was born in Brenham, TX on August 30, 1986. He received his Associates in Science from Blinn College in Brenham. He obtained his Bachelors of Biology from Texas A&M University in College Station, TX. George worked in Dr. Jennifer Bizon and Dr. Barry Setlow's laboratory at Texas A&M Psychology Department and the University of Florida McKnight Brain Institute for 3 years where he obtained his first publication (*Neurobiology of Aging*); in addition, he has had his work presented at over 11 national and international conferences. George enrolled as a graduate student at The University of Texas Health Science Center at Houston Graduate School of Biomedical Sciences in August 2011. He joined Dr. Claudio Soto's research laboratory to carry out his dissertation work.